DOI: 10.1002/chem.200500492

Electro- and Magnetocommunication in [5,5]Ditrovacenyls, $[(\eta^7\text{-}C_7H_7)V(\eta^5\text{-}C_5H_4\text{-}X\text{-}\eta^5\text{-}C_5H_4)V(\eta^7\text{-}C_7H_7)]$, Mediated by the Spacers X = (*Z*)−CH=CH−, (*E*)−CH=CH−, >C=CH₂, −CH₂CH₂−, and −CH₂−**

Christoph Elschenbroich,*[a] Jörn Plackmeyer,[b] Mathias Nowotny,[a] Andreas Behrendt,[a] Klaus Harms,[a] Jürgen Pebler,[a] and Olaf Burghaus[a]

Abstract: Five new paramagnetic dinuclear complexes containing [5]trovacenyl groups, $(\eta^7\text{-}C_7H_7)V(\eta^5\text{-}C_5H_4\text{-})$, have been prepared and characterized, including by single-crystal X-ray diffraction. As intervening spacers, ethenediyl units in the geminal and vicinal (*Z*)- and (*E*)-bridging modes as well as methanediyl and ethanediyl units have been included with the aim of studying their propensity to transmit electric and magnetic information. It is found that redox splitting of consecutive electron-transfer steps is resolved for reduction (0→1−→2−) only, unsaturation of the C_2 bridge not being requisite, since the $-CH_2CH_2-$ spacer also gives rise to a small redox splitting. Magnetic communication is quantified in terms of the exchange coupling constant *J*, accessible from the EPR hyperfine pattern in solution and from magnetic susceptometry in the solid state. The results obtained from these methods generally differ; this fact is not surprising in view of conformational differences in the respective states of aggregation. It is concluded that orientation-dependent mechanisms of spin–spin interactions (π-orbital overlap, hyperconjugation) contribute extensively although, as implied by sizeable *J* values for $-CH_2-$ and $-C_2H_4-$ linked di[5]trovacenyl groups, coupling mediated by the σ-orbital chain must also be considered.

Keywords: magnetic properties · organic spacers · redox chemistry · sandwich complexes · vanadium

Introduction

It is almost a truism now that, after the inception of the Creutz–Taube ion $[(H_3N)_5Ru(pyrazine)Ru(NH_3)_5]^{5+}$ in 1969,[2] studies of mixed/intermediate valence complexes and their role in intramolecular electro- and magnetocommunication have become vital parts of contemporary research in coordination chemistry.[3] Much effort has been invested in the elucidation of the role that the nature of the spacer between two interacting units plays in governing the redox splitting between successive electron-transfer steps (electrocommunication) and the sign and magnitude of exchange coupling of unpaired spins (magnetocommunication). Our own contribution to the field consists of the use of sandwich complex units, trovacene $[(\eta^7\text{-}C_7H_7)V(\eta^5\text{-}C_5H_5)]$ (**1**)[4] in particular, as a probe of electrochemical and magnetic properties. Paramagnetic trovacene lends itself admirably to this type of investigation, since it possesses a nondegenerate $^2A_1$ ground state giving rise to well-resolved ^{51}V hyperfine structure in EPR spectra; in addition it features two adjacent reversible redox couples ($\mathbf{1}^{+/0/-}$) and can be lithiated regioselectively at the cyclopentadienyl ring, thereby rendering a variety of derivatives accessible. In the past we have described, amongst others, [5]trovacenyl carboxylic acid $[(C_7H_7)V(C_5H_4\text{-}COOH)]$, which features exchange coupling in the hydrogen-bonded dimer $(\mathbf{2}^{\bullet})_2$;[5] the isomers [5-5]bitrovacene $\mathbf{3}^{\bullet\bullet}$[6] and [7-7]bitrovacene $\mathbf{4}^{\bullet\bullet}$,[7] which display a pronounced difference in the extent of exchange coupling; and the pair of [5,5]bitrovacenes $\mathbf{5}^{\bullet\bullet}$ and $\mathbf{6}^{\bullet\bullet}$, which were conceived in order to assess the influence a side-on versus a head-on π-stacked disposition of two trovacene units may exert on intramolecular interactions.[8] A very recent study addressed the role of ethynyl- and butadiynyl units in inter-

---

[a] Prof. Dr. C. Elschenbroich, Dr. M. Nowotny, Dr. A. Behrendt,
K. Harms, Prof. Dr. J. Pebler, Dr. O. Burghaus
Fachbereich Chemie, Philipps-Universität Marburg
Hans-Meerwein-Strasse, 35032 Marburg (Germany)
Fax: (+49) 6421-282-5653
E-mail: eb@chemie.uni-marburg.de

[b] Dr. J. Plackmeyer
Institut für Physikalische und Theoretische Chemie
Universität Frankfurt, Marie-Curie-Str. 11
60439 Frankfurt/Main (Germany)

[**] Trovacene Chemistry, Part 10; for Part 9 see reference [1].

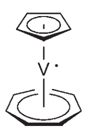

1$^{\bullet}$

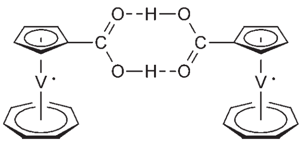

(**2**$^{\bullet}$)$_2$

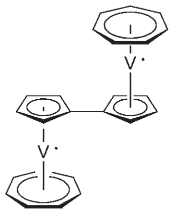

3$^{\bullet\bullet}$

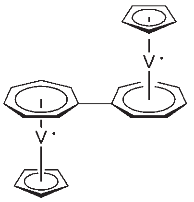

4$^{\bullet\bullet}$

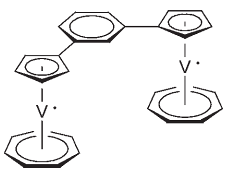

5$^{\bullet\bullet}$

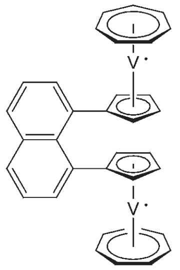

6$^{\bullet\bullet}$

[5]trovacenyl communication.[1] The present paper focusses on ethylene as a spacer: the question raised is how the three different ways (1,1-, (*E*)-1,2-, and (*Z*)-1,2-) of connecting two [5]trovacenyl groups to ethylene are reflected in the redox properties and the magnetic behavior of the products? The synthesis and properties of the important intermediates acetyl[5]trovacene (**8**$^{\bullet}$) and formyl[5]trovacene (**12**$^{\bullet}$), and that of the reference molecule vinyl[5]trovacene (**13**$^{\bullet}$) will also be described. Finally, 1,2-di([5]trovacenyl)ethane (**15**$^{\bullet\bullet}$) and di([5]trovacenyl)methane (**17**$^{\bullet\bullet}$) have been included in the series with the intent of probing the charge- and spin-mediating properties of saturated spacers. It should be mentioned that diamagnetic di(ferrocenyl)ethenes[9] and di(ruthenocenyl)ethenes[10] have been prepared previously with similar aims in mind. The open-shell nature of trovacene and the attendant exchange coupling in dinuclear complexes represent an additional phenomenon to be exploited in a study of intramolecular interactions.

Results and Discussion

Syntheses: Since for the generation of ethylene-linked bitrovacenes the McMurry type reductive coupling appeared most promising, syntheses of the requisite mononuclear carbonyl–trovacene precursors was called for. Scheme 1 depicts the synthesis of acetyl[5]trovacene (**8**$^{\bullet}$) and its conversion to the target compounds (*Z*)-**9**$^{\bullet\bullet}$, (*E*)-**9**$^{\bullet\bullet}$, and **11**$^{\bullet\bullet}$. Acetyl[5]trovacene (**8**$^{\bullet}$) rather than formyl[5]trovacene (**12**$^{\bullet}$) was employed in the McMurry coupling process, because aldehydes are known to yield (*E*)-alkenes almost exclusivley,[12] while ketones lead to a mixture of *E* and *Z* isomers, which are the target compounds in our study. In fact, we isolated the isomers (*Z*)-**9**$^{\bullet\bullet}$ and (*E*)-**9**$^{\bullet\bullet}$ in a 2:1 ratio. Separation was based on the lower solubility of the *E* isomer in toluene and on its stronger retention in column chromatography. 1,1-Bis([5]trovacenyl)ethene (**11**$^{\bullet\bullet}$) was conventionally synthesized by Wittig olefination of bis([5](trovacenyl)ketone. However, the low-yield access to the latter ketone[13] disfavored this approach and, instead, the path involving dehydration of the tertiary carbinol **10**$^{\bullet\bullet}$ was followed. This synthesis has precedent in the preparation of vinylferrocene from acetylferrocene and $LiAlH_4$[14] and of 1,1-diferrocenylethene from diferrocenylketone and CH_3MgBr;[15] in both cases dehydration of the respective ferrocenylcarbinol forms the terminal step.

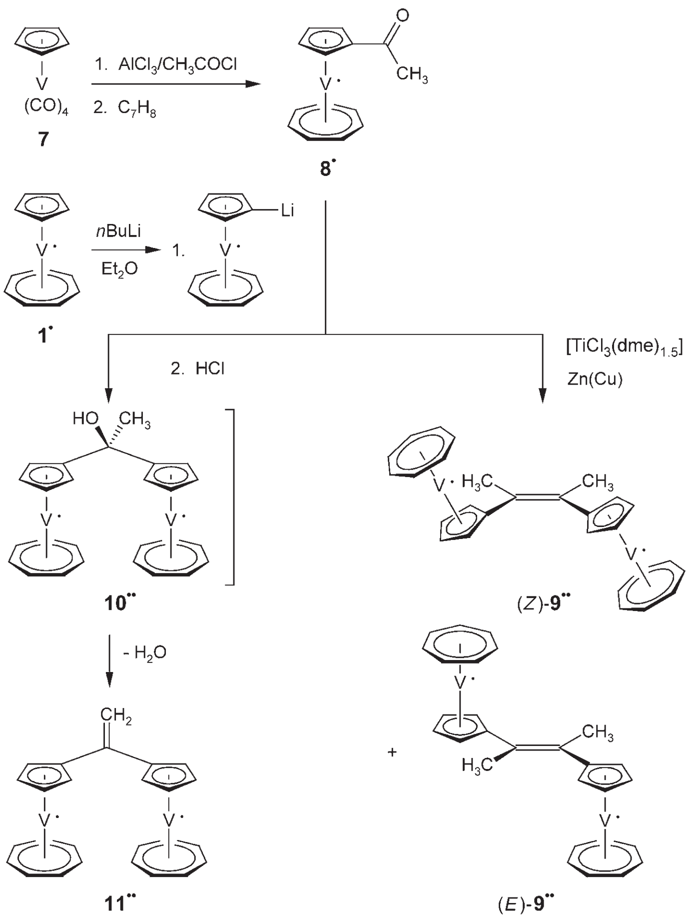

Scheme 1.

The preparation of formyl[5]trovacene (**12**$^{\bullet}$),[1] its titanium-mediated carbonyl olefination by means of $(C_5H_5)_2Ti(CH_3)_2$[11a] to yield vinyl[5]trovacene (**13**$^{\bullet}$), and reductive coupling to 1,2-di([5]trovacenyl)ethane (**15**$^{\bullet}$) are outlined in Scheme 2. For the synthesis of **17**$^{\bullet\bullet}$, it proved advantageous to prepare the bridging ligand dicyclopentadienylmethane

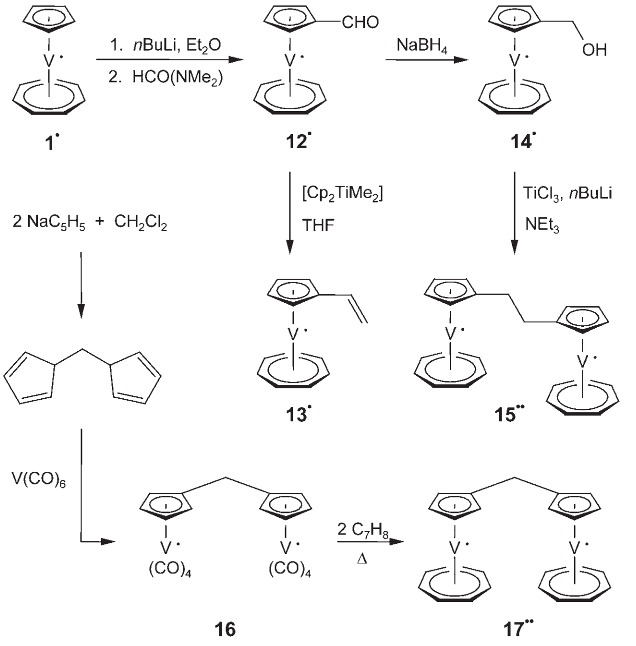

Scheme 2.

prior to formation of the trovacene units in the standard way via the intermediate **16**.

Structural studies: Crystals suitable for X-ray diffraction could be grown for the compounds (*E*)-**9**$^{\cdot\cdot}$, (*Z*)-**9**$^{\cdot\cdot}$, **11**$^{\cdot\cdot}$, **12**$^{\cdot}$, and **15**$^{\cdot\cdot}$; graphical representations of the molecular structures are shown in Figure 1 and selected bond lengths and angles are given in Table 1.

Compared to the parent complex **1**$^{\cdot}$,[16] no significant structural deviations are observed for the trovacenyl units of the derivatives reported herein, except for a slight (≈2 pm) elongation of the intraring C$_{ipso}$–C bonds of the substituted cyclopentadienyl ligand. In a valence bond picture, this may be attributed to the participation of resonance structures with C$_{ipso}$–C single bonds, effected by π-donation from the substituent (alkenyl, formyl). Consequently, the elongation is absent in the structure of complex **15**$^{\cdot\cdot}$, which features a saturated ethano bridge.

In the crystals of formyl[5]trovacene (**12**$^{\cdot}$)[1] rotational disorder of the η^5-C$_5$H$_4$C(O)H ligand was encountered as depicted in Figure 1. In both forms, the formyl substituents are coplanar with the cyclopentadienyl ring. For the discussion of intramolecular interactions in the dinuclear complexes the most pertinent structural aspect is, of course, the mutual disposition of the π-systems of η-C$_5$H$_4$ and bridging groups. However, it must be stressed at the outset that solid-state structural information is strictly applicable only in discussions of bulk magnetic susceptibility data obtained form microcrystalline samples. They may offer hints as to favored conformations in fluid solution, but they will not tell the whole story since nonrigidity in solution may affect the communication between the sandwich cores and the bridging units. With regard to the central ethene bridge, the [5]trovacenyl units adopt *anti* dispositions in the vicinal derivatives (*E*)-**9**$^{\cdot\cdot}$ and (*Z*)-**9**$^{\cdot\cdot}$, but a *syn* orientation in geminal **11**$^{\cdot\cdot}$. The lengths of 1.48 Å displayed by the C$_{ipso}$–C$_{bridge}$ bonds point to conjugation between sp^2-hybridized carbon atoms. Varying angles between the C=C double-bond vector of the bridging unit and the cyclopentadienyl ligand plane to which it is connected are encountered. For the (*E*)-**9**$^{\cdot\cdot}$ isomer, a torsional angle of 23.0° is found, whereas for the (*Z*)-**9**$^{\cdot\cdot}$ isomer it amounts to 36.6°. The geminal isomer **11**$^{\cdot\cdot}$ possesses two sterically inequivalent [5]trovacenyl groups in which the aforementioned torsion angles are 5.0° and 38.6°, respectively. For steric reasons, it is impossible for both [5]trovacenyl units to maintain maximal conjugation with the C=C double bond of the bridge, leading to severe torsion of one of them with regard to the C$_{ipso}$–C$_\alpha$ bond. In the following sections, the structural features of the trovacene derivatives in the crystal will be used in discussions of electrochemical and magnetic properties of the respective species in solution. While this is not strictly correct, justification stems from the notion that conformations encountered in the crystal may also be the preferred ones in fluid solution.

Redox properties: Figure 2 shows the waves obtained from subjecting the complexes (*Z*)-**9**$^{\cdot\cdot}$, (*E*)-**9**$^{\cdot\cdot}$, **11**$^{\cdot\cdot}$, **15**$^{\cdot\cdot}$, and **17**$^{\cdot\cdot}$ to cyclic voltammetry; the pertaining data are given in the caption. With regard to the potentials at which oxidations and reductions occur, the isomeric dinuclear complexes (*Z*)-**9**$^{\cdot\cdot}$ and (*E*)-**9**$^{\cdot\cdot}$ closely resemble each other; consequently, the redox splittings $\delta E_{1/2}$, which define the potential difference between subsequent redox processes at the two central metal atoms present, are practically identical. Whereas the redox splittings $\delta E_{1/2}$ (2+/+; +/0) for the oxidation steps are unresolved in the cyclovoltammetric traces, they are clearly discernable for the reduction steps as $\delta E_{1/2}$ (0/−; −/2−). The fact that electrocommunication in dinuclear complexes, as expressed by the redox splittings $\delta E_{1/2}$, is generally larger for reductions than for oxidations has been commented on.[5] Despite closer proximity of the trovacenyl units in the isomer (*Z*)-**9**$^{\cdot\cdot}$ relative to (*E*)-**9**$^{\cdot\cdot}$, redox splitting $\delta E_{1/2}$ is somewhat smaller for the former. This must be traced to the more extensive twisting of the trovacenyl groups of (*Z*)-**9**$^{\cdot\cdot}$ in relation to the bridging ethene unit and the attendant decrease of π-conjugation. Accordingly, transmission of electronic effects will be attenuated. Therefore, the conclusion that in the analogous di(ferrocenyl)ethene compounds intramolecular electronic interaction is dominated by coulomb repulsion[9d] warrants reconsideration. The influence that π-conjugation exerts on the degree of electrocommunication may also be gleaned from the electrochemical properties of the geminal isomer **11**$^{\cdot\cdot}$. Even though the number of C(sp^2) atoms in the bridge is smaller, $\delta E_{1/2}$ (2+/+; +/0, **11**$^{\cdot\cdot}$) fails to be resolved and the value $\delta E_{1/2}$ (0/−; −/2−; **11**$^{\cdot\cdot}$) falls short of that observed for the C$_2$-separated dinuclear complexes (*Z*)-**9**$^{\cdot\cdot}$ and (*E*)-**9**$^{\cdot\cdot}$. This comes as no surprise in view of the fact that the angle of twist between the η^5-C$_5$H$_4$ and the bridging ethene unit is maximal for **11**$^{\cdot\cdot}$. Yet, electrocommunication should not be traced to π-conjugation exclusive-

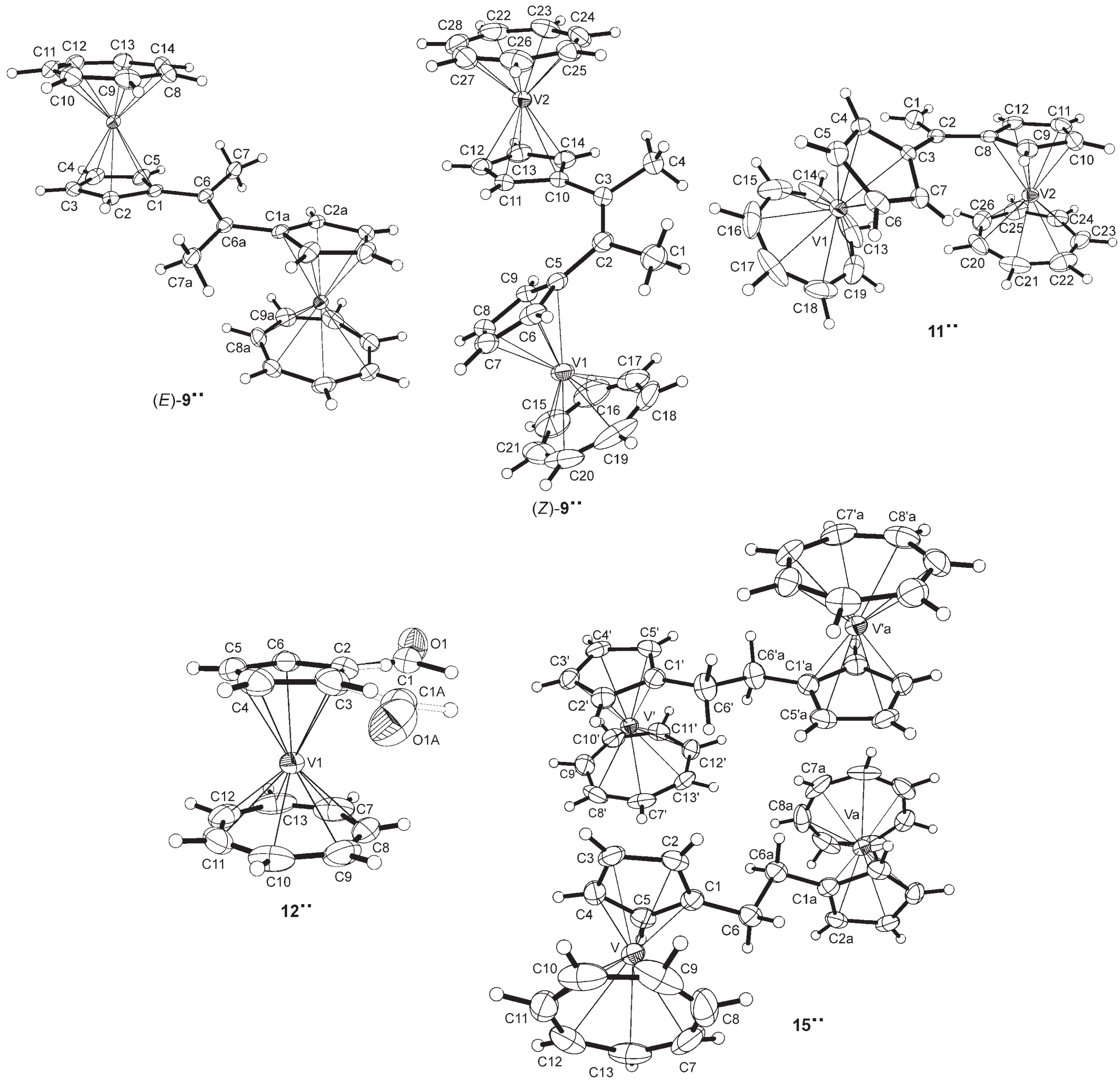

Figure 1. Molecular structures of (*E*)-$\mathbf{9}^{\cdot\cdot}$, (*Z*)-$\mathbf{9}^{\cdot\cdot}$, $\mathbf{11}^{\cdot\cdot}$, $\mathbf{12}^{\cdot}$, and $\mathbf{15}^{\cdot\cdot}$ in the crystal (XP drawing and numbering scheme; ellipsoids are drawn at the 50% level).

ly, as the electrochemical behavior of 1,2-di([5]trovacenyl)ethane $\mathbf{15}^{\cdot\cdot}$ demonstrates; although the trovacenyl units in $\mathbf{15}^{\cdot\cdot}$ are separated by a saturated $-CH_2-CH_2-$ spacer, a small but significant redox splitting $\delta E_{1/2}$ (0/−; −/2−, $\mathbf{15}^{\cdot\cdot}$) is observed. Electrocommunication therefore is also transmitted by a sequence of σ bonds or through C−H/π hyperconjugation. In this context, the reader may recall early work on diferrocenyl alkanes $[Fc(CH_2)_nFc]$, which lead to the redox splittings $\delta E_{1/2}$ (2+/+; +/0) = 300 ($n=0$), 170 ($n=1$), 40 mV ($n=2$).[17] For the di([5]trovacenyl)analogues $\mathbf{3}^{\cdot}$, $\mathbf{17}^{\cdot\cdot}$, and $\mathbf{15}^{\cdot\cdot}$, the gradations $\delta E_{1/2}$ (2+/+; +/0) = 147 mV ($n=0$), not resolved ($n=1$), not resolved ($n=2$); and $\delta E_{1/2}$ (0/−; −/2−) = 224 ($n=0$), 100 ($n=1$), 82 mV ($n=2$) apply.

Apart from providing information on the extent of intermetallic communication, redox splittings $\delta E_{1/2}$ also serve in calculations of comproportionation constants K_{con} according to the relation $\log K_{con} = 16.9\,\delta E_{1/2}$ at 298 K.[18] Applied to the systems under study here, for K_{con} the values 160 ((*Z*)-$\mathbf{9}^{\cdot-}$), 800 ((*E*)-$\mathbf{9}^{\cdot-}$), 20 ($\mathbf{15}^{\cdot-}$) and 50 ($\mathbf{17}^{\cdot-}$) are derived. Thus, whereas upon oxidation equilibrium mixtures will be ob-

Table 1. Selected interatomic distances, bond lengths [Å], and angles [°] for (E)-$\mathbf{9}^{\bullet\bullet}$, (Z)-$\mathbf{9}^{\bullet\bullet}$, $\mathbf{11}^{\bullet\bullet}$, $\mathbf{12}^{\bullet}$, and $\mathbf{15}^{\bullet\bullet}$.

(E)-$\mathbf{9}^{\bullet\bullet}$							
V−VA	7.6630(23)	V−C(Cp) av	2.2623(15)	V−Cp cent	1.9101(34)	C−C(Cp) av	1.4185(42)
V−C(Tr) av	2.1880(16)	V−Tr cent	1.4629	C−C(Tr) av	1.4013(37)	C1−C2	1.435(2)
C2−C3	1.414(2)	C3−C4	1.409(3)	C4−C5	1.417(2)	C1−C5	1.432(2)
C1−C6	1.488(2)	C6−C6A	1.356(3)	C6−C7	1.513(2)		
C1-C6-C7	113.49(13)	C6A-C6-C1	124.01(17)	C6A-C6-C7	122.47(17)		
C2-C1-C6-C6A	23.0(3)	C5-C1-C6-C6A	157.58(18)	C5-C1-C6-C7 20.2(2)	C2-C1-C6-C7	159.16(15)	
(Z)-$\mathbf{9}^{\bullet\bullet}$							
V1−V2	7.1678(7)	V1−C(Cp) av	2.2648(19)	V1−Cp cent	1.9192(10)	C−C(Cp) av	1.4142(13)
V1−C(Tr) av	2.1735(3)	V1−Tr cent	1.4628	C−C(Tr) av	1.3922(20)	C5−C6	1.431(3)
C6−C7	1.402(3)	C7−C8	1.404(3)	C8−C9	1.413(3)	C5−C9	1.421(3)
V2−C(Cp) av	2.2657(19)	V2−Cp cent	1.9189(10)	C−C(Cp) av	1.4180(13)	V2−C(Tr) av	2.1845(2)
V2−Tr cent	1.4671	C−C(Tr) av	1.4038(13)	C10−C11	1.425(3)	C10−C14	1.428(3)
C11−C12	1.417(3)	C12−C13	1.409(3)	C13−C14	1.410(3)	C2−C5	1.480(3)
C10−C3	1.482(3)	C2−C3	1.347(3)	C3−C4	1.514(3)	C2−C1	1.516(3)
C3-C2-C5	124.42(17)	C3-C2-C1	119.97(19)	C5-C2-C1	115.61(18)	C2-C3-C10	124.34(18)
C2-C3-C4	119.52(18)	C10-C3-C4	116.07(17)				
C1-C2-C3-C4	7.1(3)	C1-C2-C3-C10	176.14(19)	C5-C2-C3-C4	173.03(17)	C5-C2-C3-C10	3.7(3)
C1-C2-C5-C9	143.5(2)	C3-C2-C5-C6	139.3(2)	C3-C2-C5-C9	36.6(3)	C1-C2-C5-C6	40.6(3)
C2-C3-C10-C11	37.5(3)	C2-C3-C10-C14	139.5(2)	C4-C3-C10-C11	145.66(19)	C4-C3-C10-C14	37.3(3)
$\mathbf{11}^{\bullet\bullet}$							
V1−V2	5.6747(10)	V1−C(Cp) av	2.272(4)	V1−Cp cent	1.927(2)	C−C(Cp) av	1.4174(28)
V1−C(Tr) av	2.171(7)	V1−Tr cent	1.469	C−C(Tr) av	1.3877(47)	C3−C4	1.424(6)
C4−C5	1.405(7)	C5−C6	1.409(7)	C6−C7	1.421(6)	C3−C7	1.425(6)
V2−C(Cp) av	2.267(5)	V2−Cp cent	1.919(2)	C−C(Cp) av	1.4220(29)	V2−C(Tr) av	2.180(6)
V2−Tr cent	1.463	C−C(Tr) av	1.4013(32)	C8−C9	1.430(6)	C9−C10	1.417(7)
C10−C11	1.406(8)	C11−C12	1.417(7)	C8−C12	1.437(6)	C1−C2	1.330(6)
C2−C3	1.487(6)	C2−C8	1.478(6)				
C1-C2-C8	120.2(4)	C1-C2-C3	120.8(4)				
C1-C2-C3-C4	38.6(6)	C1-C2-C3-C7	145.5(5)	C8-C2-C3-C4	135.9(4)	C8-C2-C3-C7	39.9(6)
C1-C2-C8-C9	171.6(5)	C1-C2-C8-C12	5.0(7)	C3-C2-C8-C9	3.0(6)	C3-C2-C8-C12	179.6(4)
$\mathbf{12}^{\bullet}$							
V1−C(Cp) av	2.261(2)	C−C(Cp) av	1.408(4)	V1−C(Tr) av	2.171(3)	C−C(Tr) av	1.393(5)
O1−C1	1.214(6)	C1−C2	1.407(6)	C1A−O1A	1.208(6)	C1A−C3	1.489(6)
C2−C6	1.416(3)	C2−C3	1.421(3)	C3−C4	1.403(4)	C4−C5	1.399(4)
C5−C6	1.402(4)						
O1-C1-C2	121.8(5)	O1A-C1A-C3	119.9(5)				
O1-C1-C2-C6	2.1(6)	O1-C1-C2-C3	−172.1(4)	O1A-C1A-C3-C4	−8.9(6)	O1A-C1A-C3-C2	−179.2(4)
$\mathbf{15}^{\bullet\bullet}$							
V−VA	7.9725(10)	V−C(Cp) av	2.255(3)	V−Cp cent	1.9079(15)	C−C(Cp) av	1.4141(20)
V−C(Tr) av	2.172(4)	V−Tr cent	1.4702(16)	C−C(Tr) av	1.3879(22)	C1−C6	1.511(4)
C6−C6A	1.530(6)	V′−V′A	7.2574(9)	V′−C(Cp) av	2.256(3)	V′−Cp cent	1.9120(16)
C−C(Cp) av	1.4097(21)	V′−C(Tr) av	2.181(4)	V′−Tr cent	1.4669(15)	C−C(Tr) av	1.4013(19)
C1′−C6′	1.511(4)	C6′−C6′A	1.520(6)				
C1-C6-C6A	112.4(3)	C2-C1-C6	126.6(3)	C5-C1-C6	126.7(3)	C1′-C6′-C6′A	114.3(4)
C2′-C1′-C6′	124.7(3)	C5′-C1′-C6′	128.1(3)				
C2-C1-C6-C6A	−76.0(5)	C5-C1-C6-C6A	102.8(4)	C2′-C1′-C6′-C6′A	163.8(4)	C5′-C1′-C6′-C6′A	−20.7(6)

tained which contain the three species (0/0), (0/+), and (+/+) in similar concentrations, reduction should, in principle, allow the generation of the mixed/intermediate valence species (Z)-$\mathbf{9}^{\bullet-}$ and (E)-$\mathbf{9}^{\bullet-}$ virtually uncontaminated by isovalent (0/0) and (−/−). Experimental problems of performing controlled potential electrolyses at the very negative potentials required and subsequent separation of the mixed/intermediate valence salts R_4N^+ $(0/-)^{\bullet-}$ from supporting electrolyte has as yet precluded the isolation of (Z)-$\mathbf{9}^{\bullet-}$, (E)-$\mathbf{9}^{\bullet-}$, $\mathbf{11}^{\bullet-}$, $\mathbf{15}^{\bullet-}$, and $\mathbf{17}^{\bullet-}$. This is unfortunate because access to the mixed/intermediate valence species could provide an estimate of the electron coupling term V_{ab} from the energy and width at half-maximum of the vanadium–vanadium intervalence transition and the intervanadium distance by employing the Hush equation.[19] The possibility of correlating the electron-transfer matrix element V_{ab} (a one-electron quantity) with the exchange-coupling parameter J (a two-electron quantity) could be revealing and this question has already been addressed.[20]

EPR spectroscopy and magnetic susceptibility: Whereas the EPR spectra of the mononuclear complexes $\mathbf{8}^{\bullet}$, $\mathbf{12}^{\bullet}$, $\mathbf{13}^{\bullet}$, and $\mathbf{14}^{\bullet}$ do not invite much comment, those of the binuclear species (Z)-$\mathbf{9}^{\bullet\bullet}$, (E)-$\mathbf{9}^{\bullet\bullet}$, $\mathbf{11}^{\bullet\bullet}$, $\mathbf{15}^{\bullet\bullet}$, and $\mathbf{17}^{\bullet\bullet}$ warrant detailed discus-

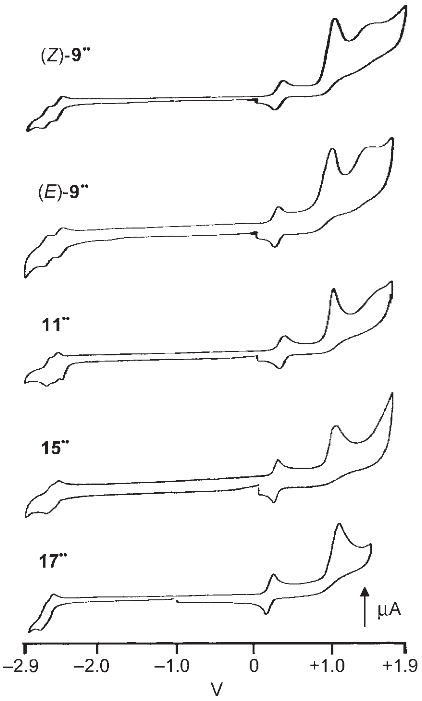

Figure 2. Cyclic voltammograms for (Z)-**9**$^{\cdot\cdot}$, (E)-**9**$^{\cdot\cdot}$, **11**$^{\cdot\cdot}$, **15**$^{\cdot\cdot}$, and **17**$^{\cdot\cdot}$ in DME/0.1 M n-Bu_4NClO_4 at $T=-40\,°C$ and $v=100\,mV\,s^{-1}$ versus SCE. Additional peak potentials E_p (reversibilitiy criteria not applicable): Compound (Z)-**9**$^{\cdot\cdot}$: $E_{1/2}(2+/+)=0.31$ V, $\Delta E_p=77$ mV, $r=1$; $E_{1/2}(+/0)=0.25$ V, $\Delta E_p=62$ mV, $r=1$; $E_{pa}=1.06$, 1.53 V, $E_{1/2}(0/-)=-2.48$ V, $\Delta E_p=56$ mV, $r=0.7$; $E_{1/2}(-/2-)=-2.61$ V, $\Delta E_p=40$ mV, $r=0.85$; $K_{con}=160$. Compound (E)-**9**$^{\cdot\cdot}$: $E_{1/2}(2+/+)=0.27$ V, $\Delta E_p=64$ mV, $r=1$; $E_{1/2}(+/0)=0.27$ V, $\Delta E_p=64$ mV, $r=1$; $E_{pa}=0.94$, 1.42 V; $E_{1/2}(0/-)=-2.43$ V, $\Delta E_p=57$ mV, $r=0.5$; $E_{1/2}(-/2-)=-2.60$ V, $\Delta E_p=60$ mV, $r=0.8$; $K_{con}=800$. Compound **11**$^{\cdot\cdot}$: $E_{1/2}(2+/0)=0.31$ V, $\Delta E_p=88$ mV, $r=1$; $E_{pa}=1.06$ V; $E_{pc}=-2.43$ V; $E_{1/2}(-/2-)=-2.50$ V, $\Delta E_p=79$ mV, $r=0.7$; $E_{1/2}(2\text{-}/3\text{-})=-2.59$ V, $\Delta E_p=70$ mV, $r=0.9$. Compound **15**$^{\cdot\cdot}$: $E_{1/2}(2+/0)=0.22$ V, $\Delta E_p=64$ mV, $r=1$; $E_{pa}=1.0$ V; $E_{1/2}(0/-)=-2.51$ V, $\Delta E_p=69$ mV, $r=1$; $E_{1/2}(-/2-)=-2.59$ V, $\Delta E_p=75$ mV, $r=1$; $K_{con}=20$. Compound **17**$^{\cdot\cdot}$: $E_{1/2}(2+/0)=0.19$ V, $\Delta E_p=104$ mV, $r=1$; $E_{pa}=1.04$ V; $E_{1/2}(0/-)=-2.46$ V, $\Delta E_p=68$ mV, $r=1$; $E_{1/2}(-/2-)=-2.56$ V, $\Delta E_p=64$ mV, $r=1$; $K_{con}=50$.

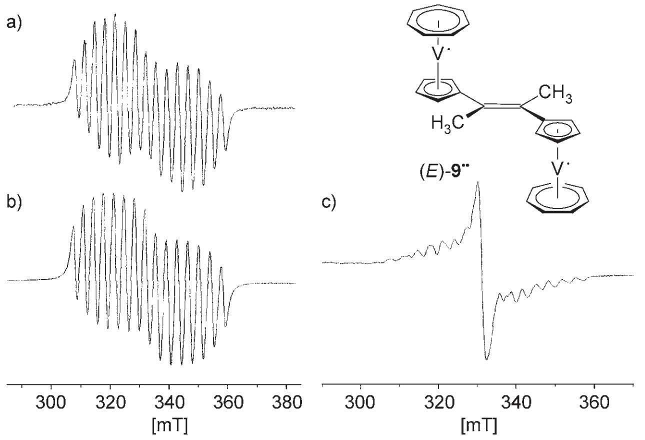

Figure 3. EPR spectra (X-band) of (E)-**9**$^{\cdot\cdot}$ in toluene: a) in fluid solution, $T=340$ K; b) simulated spectrum, $\langle g\rangle=1.9810$, $a(^{51}V)=-7.19$ mT, $|J|=1.017\,cm^{-1}$; c) in rigid solution, $T=142$ K.

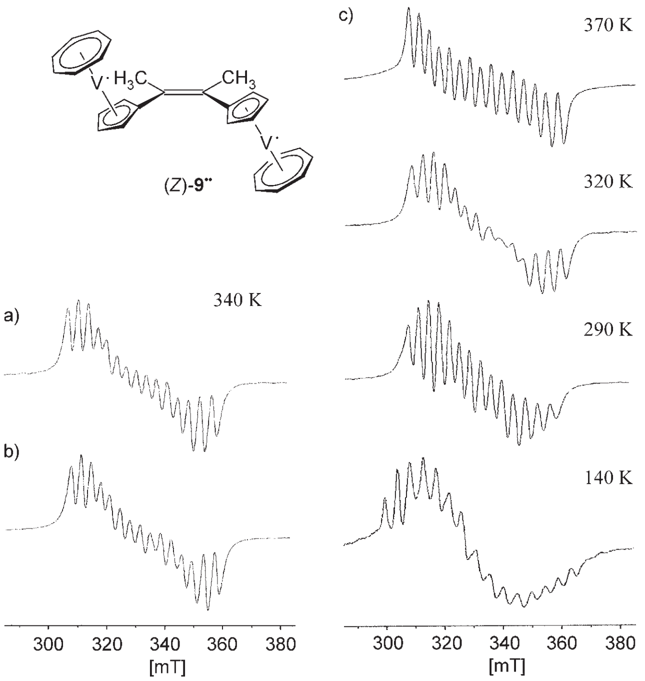

Figure 4. EPR spectra (X-band) of (Z)-**9**$^{\cdot\cdot}$ in toluene: a) in fluid solution, $T=340$ K; b) simulated spectrum, $\langle g\rangle=1.9824$, $a(^{51}V)=-7.09$ mT, $|J|=0.052\,cm^{-1}$; c) in fluid solution at various temperatures and in rigid solution, $T=140$ K.

sion, since they deal with the principal concern of this study (Figures 3–7, respectively). In all five cases, ^{51}V hyperfine splitting in the isotropic EPR spectra in fluid solution signalizes exchange coupling of the two unpaired electrons centered at the vanadium nuclei; 15 lines arise that are separated by approximately half the coupling constant $a(^{51}V)$ of the mononuclear parent complex **1**$^{\cdot}$. The hyperfine patterns display significant differences with regard to intensities and line shapes, which can be used to determine the exchange coupling constant J by means of computer simulation.[21] This procedure leads to the following gradation of $|J|$ (cm^{-1}, 340 K): >1.50 **17**$^{\cdot\cdot}$ > 1.20 **11**$^{\cdot\cdot}$ > 1.02 (E)-**9**$^{\cdot\cdot}$ > 0.52 **15**$^{\cdot\cdot}$ > 0.05 (Z)-**9**$^{\cdot\cdot}$. The isotropic EPR spectrum of **17**$^{\cdot\cdot}$ fails to display deviations from the fast exchange case; the 15 hyperfine components obey the intensity distribution 1:2:3:4:5:6:7:8:7:6:5:4:3:2:1. Concordantly, **17**$^{\cdot\cdot}$ is the only biradical in the series studied that exhibits an electron magnetic spin quantum number $\Delta m_s=2$ half-field transition. It may come as a surprise that separation by an sp^3 carbon atom in **17**$^{\cdot\cdot}$ fails to significantly attenuate the spin–spin exchange interaction of the two trovacene units relative to that in spacer-free **3**$^{\cdot\cdot}$. One must bear in mind, however, that *ortho* hydrogen compression strain will cause **3**$^{\cdot\cdot}$ to adopt a rotameric form in solution in which the cyclopentadienyl π-perimeters are orthogonal. In contrast, in **17**$^{\cdot\cdot}$ the most favorable conformation due to C(sp^3) imposed tilt of the sandwich axes leads to finite overlap of the neighboring Cp π-electron systems, which may assist through space spin–spin exchange coupling. The relatively large value for **11**$^{\cdot\cdot}$ is plausible, since in this complex, the two [5]trovacenyl units are

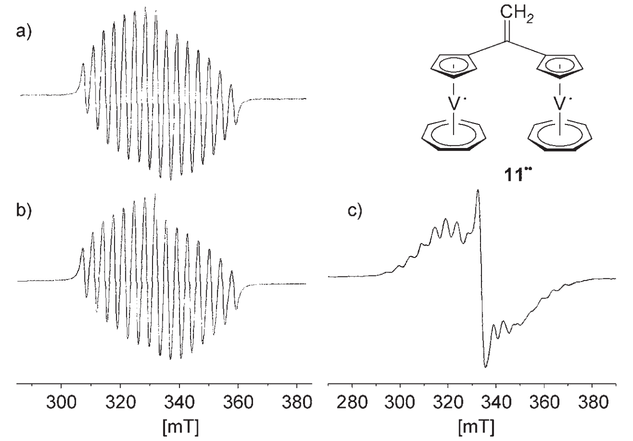

Figure 5. EPR spectra (X-band) of $\mathbf{11}^{\bullet\bullet}$ in toluene: a) in fluid solution, $T=340$ K; b) simulated spectrum, $<g>=1.9799$, $a(^{51}V)=-7.23$ mT, $|J|=1.202$ cm^{-1}; c) in rigid solution, $T=134$ K.

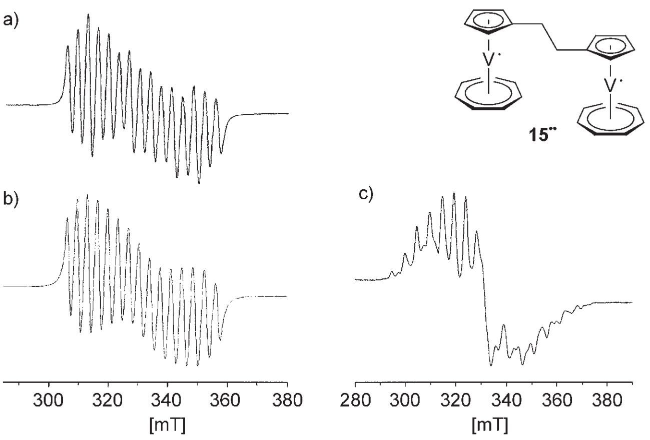

Figure 6. EPR spectra (X-band) of $\mathbf{15}^{\bullet\bullet}$ in toluene: a) in fluid solution, $T=330$ K; b) simulated spectrum, $<g>=1.9829$, $a(^{51}V)=-7.14$ mT, $|J|=0.52$ cm^{-1}; c) in rigid solution, $T=140$ K.

separated by a single C(sp^2) atom only. It must be emphasized, however, that this value is not universally representative for magnetocommunication across a single C(sp^2) spacer, since severe twist distortion of one of the [5]trovacenyl groups relative to the plane of the C(sp^2) center and the second cyclopentadienyl plane is encountered in $\mathbf{11}^{\bullet\bullet}$; this distortion curtails π-conjugation between the trovacenyl units. Stereochemically induced strongly differing degrees of coplanarity of the cyclopentadienyl and bridging ethene units in the isomeric complexes (E)-$\mathbf{9}^{\bullet\bullet}$ and (Z)-$\mathbf{9}^{\bullet\bullet}$ should in part be responsible for the dramatic difference of the exchange coupling constants J((E)-$\mathbf{9}^{\bullet\bullet}$) and J((Z)-$\mathbf{9}^{\bullet\bullet}$). Let us recall here that in (E)-$\mathbf{9}^{\bullet\bullet}$ the cyclopentadienyl rings are coplanar and the ethene bridge deviates by 22° only from the cyclopentadienyl planes. Conversely, in the isomer (Z)-$\mathbf{9}^{\bullet\bullet}$, *ortho*-H compression strain of the cyclopentadienyl protons causes more pronounced twisting of the [5]trovacenyl units relative to the ethene bridge, resulting in angles of 36.6 and 40.6°. The dihedral angle of the two cyclopentadienyl planes amounts to 37.30°. This twist distortions and the attendant decreased π-conjugation are considered to be more important than the differing intervanadium distances in affecting the J values, since these metal–metal distances differ to a small extent only, amounting to 7.66 Å for (E)-$\mathbf{9}^{\bullet\bullet}$ and 7.16 Å for (Z)-$\mathbf{9}^{\bullet\bullet}$. We stress again that the geometrical parameters obtained from X-ray diffraction certainly cannot be transferred to the structures in solution, rather they indicate a tendency for the respective minimum energy conformation and, as such, can be used in a qualitative discussion. Furthermore, the reason behind the profoundly differing values of J((E)-$\mathbf{9}^{\bullet\bullet}$) and J((Z)-$\mathbf{9}^{\bullet\bullet}$) may be a little more subtle than alluded to above. Of course, a semiquantitative explanation would have to take into account the mechanism of exchange coupling, a question we will return to after having presented the magnetic susceptibility data. At this point, however, attention should be directed to phenomena possibly related to electron–electron spin–spin interactions, namely, the electron–proton hyperfine interaction in the EPR spectrum of the vinyl radical[22a] and proton–proton scalar coupling $^3J(\mathrm{H,H})_{trans}$ and $^3J(\mathrm{H,H})_{cis}$ in the ^{1}H NMR spectra of ethylene derivatives.[22b] A common feature of these three processes is the fact that the magnitude of the E interaction exceeds that of the Z interaction, which may point at mechanistic similarity (Scheme 3).

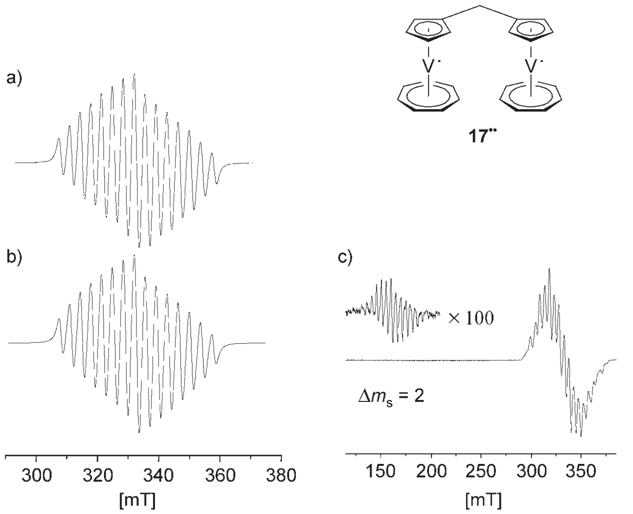

Figure 7. EPR spectra (X-band) of $\mathbf{17}^{\bullet\bullet}$ in toluene: a) in fluid solution, $T=330$ K; b) simulated spectrum, $<g>=1.9839$, $a(^{51}V)=-7.11$ mT, $|J|$ >1.5 cm^{-1}; c) in rigid solution, $T=140$ K. From the splitting of 4.98 mT in the $\Delta M_s=2$ multiplet, $A_{\perp}(^{51}V)=-9.96$ mT is derived.

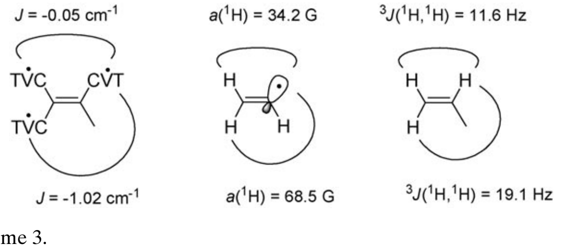

Scheme 3.

Replacing an unsaturated ethene by a saturated ethane unit in the spacer would be expected to cause quenching of intramolecular electron spin–spin interaction. Yet, 1,2-di([5](trovacenyl)ethane ($\mathbf{15}^{\bullet\bullet}$), which was shown to engage in finite electrocommunication, $\delta E_{1/2}$ (0/−; −/2−) = 82 mV, also displays sizeable intramolecular magnetic interactions, in that the analysis of the EPR hyperfine pattern yielded the value $|J|(\mathbf{15}^{\bullet\bullet}) = 0.52\ \text{cm}^{-1}$. This finding sheds light on the mechanism of exchange coupling, since it indicates that magnetic interaction can occur even in the absence of π conjugation.[23] Two variants come to mind: a) exchange coupling is transmitted by means of spin polarization of the C–C σ bonds of the $-CH_2CH_2-$ linker; b) exchange coupling is mediated by a path that utilizes hyperconjugation of the C_α–H bonds with the η^5-cyclopentadienyl π-electron system. Corroborative evidence for both paths is provided by the isotropic EPR spectra of the bis(η^6-arene)metal (d^5) species $\mathbf{18}^{\bullet+}$ and $\mathbf{19}^{\bullet+}$, which feature C_α–H bonds in sterically fixed positions (Figure 8).[24] Whereas in the radical cation [(η^{12}-[2.2]paracyclophane)chromium]$^{\bullet+}$ ($\mathbf{18}^{\bullet+}$) the β-protons are confined to the nodal plane of the ligand π-electron system, in the radical cation [bis(cyclobuta-η^6-benzene)chromium]$^{\bullet+}$ ($\mathbf{19}^{\bullet+}$) the C_α–H bond axes are almost cofacial with the ligand π orbitals. The gradation of hyperfine coupling constants a(^{1}H) given in Figure 8 demonstrates that spin density can be transferred to the methylene protons by σ-spin polarization ($\mathbf{18}^{\bullet+}$) of the C_{ipso}–C_α and C_α–H bonds as well as by hyperconjugation of the C_α–H bond with the ligand π orbitals ($\mathbf{19}^{\bullet+}$), the latter process being more effective. Both paths operate for the freely rotating methyl group in the radical cation [bis(η^6-p-xylene)chromium]$^{\bullet+}$ ($\mathbf{20}^{\bullet+}$), whereby the hyperfine coupling constant $a(12\,^1H_{Me}, \mathbf{20}^{\bullet+})$ concords with the magnitude predicted by the Heller–McConnell relationship $a(^1H_\beta) = B_0 + \cos^2\Theta B_2$[25] ($B_0$ = conformation-independent part, B_2 = conformation-dependent part, Θ angle of twist between the ligand p_z orbital and the C_α–H bond). It therefore is plausible that a conformationally flexible $-CH_2CH_2-$ spacer in the diradical $\mathbf{15}^{\bullet\bullet}$ provides an exchange coupling path. In all five cases (Z)-$\mathbf{9}^{\bullet\bullet}$, ($E$)-$\mathbf{9}^{\bullet\bullet}$, $\mathbf{11}^{\bullet\bullet}$, $\mathbf{15}^{\bullet\bullet}$, and $\mathbf{17}^{\bullet\bullet}$ exchange coupling is initiated by spin polarization of filled ligand π-orbitals by the SOMO a_1, which is an almost pure central metal d_{z^2} orbital, the π-spin density thus generated at the C_{ipso} atom then interacts with the spacer. It is the small magnitude of spin density present at C_{ipso} that renders fluid solution EPR applicable in the study of the superexchange process here, since in this way the condition for ^{51}V hyperfine structure to be informative, namely $J \leq 500\,a(^{51}V)$, is fulfilled. There have been a few other studies of exchange coupling on organometallic oligoradicals, employing the paramagnetic units $[TiCp_2]^+$,[26] [Mo(NO)Tp^{Me,Me}Cl] and [Mo(O)Tp^{Me,Me}Cl] (Tp^{Me,Me} = hydrotris(3,5-dimethylpyrazolyl)borate),[27] and $[Cp^*Fe(Ph_2P(CH_2)_2PPh_2)]^{2+}$.[28] In all these cases, the unpaired electron resides in a central metal orbital that can engage in π bonding with the orbitals of the spacer. In contrast, in the trovacene probe the singly occupied vanadium orbital is essentially a vanadium $3d_{z^2}$ function that is orthogonal to the molecular orbitals of the cyclopentadienyl ligand. Therefore, the spin densities that leak into the spacers and, correspondingly, the J values, are very small, too small for magnetic susceptometry to be applicable in most instances. Yet, they are just of the right size to lead to very characteristic ^{51}V hyperfine patterns for trovacene/spacer combinations of general interest. In Figure 9 model simulations for different J/a ratios are depicted, whereby for

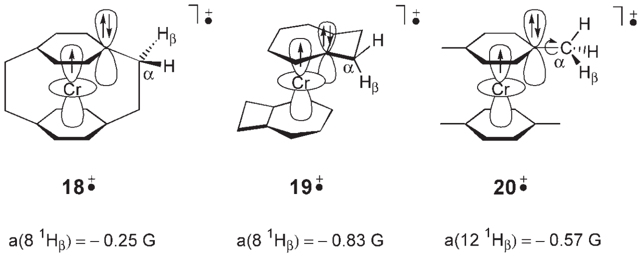

Figure 8. σ versus π spin transfer in the isotropic EPR spectra of [(η^{12}-[2.2]paracyclophane)chromium]$^{\bullet+}$ ($\mathbf{18}^{\bullet+}$), [bis(cyclobuta-η^6-benzene)chromium]$^{\bullet+}$ ($\mathbf{19}^{\bullet+}$), and [bis(η^6-p-xylene)chromium]$^{\bullet+}$ ($\mathbf{20}^{\bullet+}$).

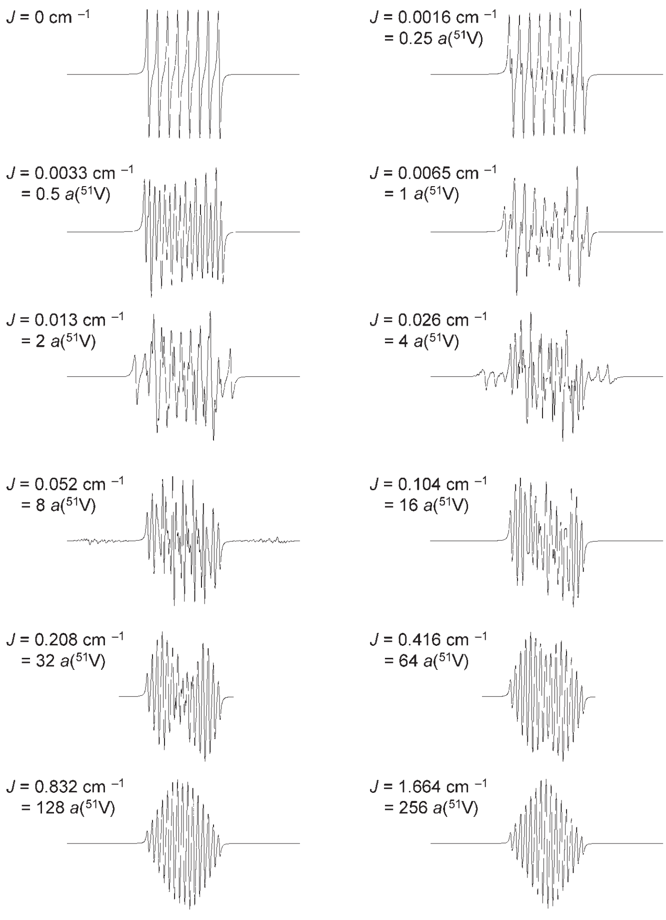

Figure 9. Model simulations of ^{51}V hyperfine patterns in EPR spectra of bitrovacenes for different J/a ratios. Reference: $|a(^{51}V, \mathbf{1}^{\bullet})| = 6.98\ \text{mT} \mathrel{\hat{=}} 0.0065\ \text{cm}^{-1}$. A constant linewidth of 2.0 mT has been assumed, that is, m_I dependency has been neglected.

$a(^{51}V)$ the value $65.4\times10^{-4}\,cm^{-1}$ has been adopted, which pertains to mononuclear trovacene, and J was varied from 0 to $1.66\,cm^{-1}$, thereby covering the ratios $0<J/a<256$. Since ^{51}V occurs in 99.75 % natural abundance, these hyperfine patterns arise unobstructed by a superimposed signal due to a nonmagnetic isotopomer and precise J values can be derived by fitting the experimental spectra. Alternatively, the simulated traces (Figure 9) can serve as finger prints in obtaining good estimates of J values by simple visual inspection.

The EPR hyperfine patterns of exchange-coupled diradicals are unaffected by the sign of J. Therefore they do not reveal whether the interaction is ferromagnetic ($J>0$) or antiferromagnetic ($J<0$). This information is available from a study of the temperature dependence of magnetic susceptibility, the respective plots for the compounds (Z)-**9**$^{\bullet\bullet}$, (E)-**9**$^{\bullet\bullet}$, **11**$^{\bullet\bullet}$, **15**$^{\bullet\bullet}$, and **17**$^{\bullet\bullet}$ are shown in Figure 10. Only in the case of **17**$^{\bullet\bullet}$ is a well-developed maximum observed that attests to $J<0$; for (E)-**9**$^{\bullet\bullet}$ and **11**$^{\bullet\bullet}$ an inflection at extremely low-temperature indicates that a maximum would form could even lower temperatures be reached. The susceptibility curves were fitted by means of the modified Bleaney–Bowers formula[29] [Eq. (1)], in which the correction term Θ for intermolecular magnetic interactions, the molar fraction ρ of residual uncoupled species, and the exchange coupling constant J are variational parameters; the other symbols have their usual meaning.

$$\chi_m = \frac{2Ng^2{\mu_B}^2}{k(T-\Theta)\left(3+\exp\left(-\frac{J}{kT}\right)\right)}(1-\rho) + \frac{Ng^2{\mu_B}^2}{2kT}\rho \qquad (1)$$

In Table 2 the values J_χ from magnetic susceptometry are listed together with the values J_{EPR} derived from the ^{51}V hy-

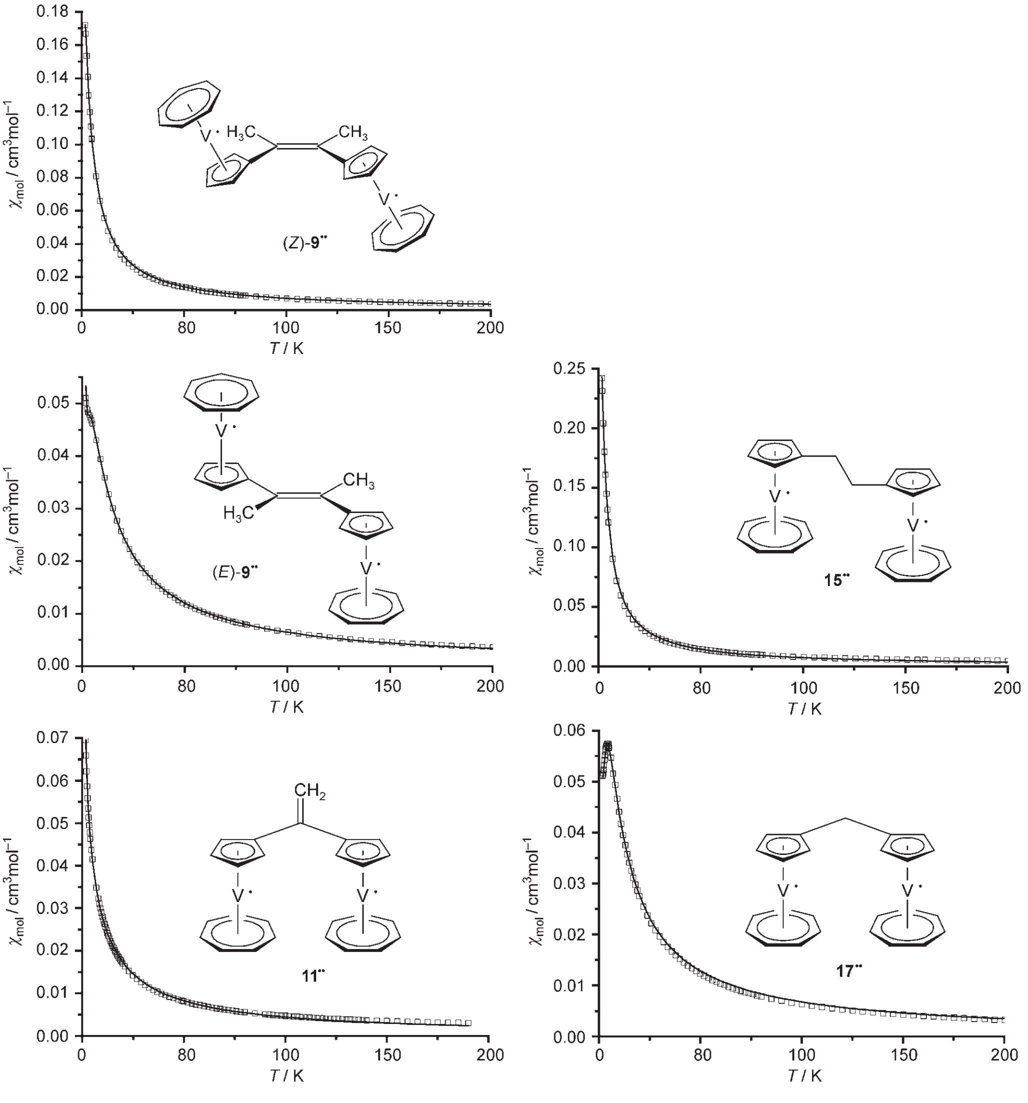

Figure 10. Magnetic susceptibility data for (Z)-**9**$^{\bullet\bullet}$, (E)-**9**$^{\bullet\bullet}$, **11**$^{\bullet\bullet}$, **15**$^{\bullet\bullet}$, and **17**$^{\bullet\bullet}$ at 10 kG in the temperature range 1.8–200 K (□). The solid lines represent the best fit to the Bleaney–Bowers expression (see text) with, compound (Z)-**9**$^{\bullet\bullet}$: $J_\chi=-2.19\,cm^{-1}$, $\Theta=-1.32$ K, and $\rho=0.24$; compound (E)-**9**$^{\bullet\bullet}$: $J_\chi=-4.65\,cm^{-1}$, $\Theta=-7.2$ K, and $\rho=0.12$; compound **11**$^{\bullet\bullet}$: $J_\chi=-2.48\,cm^{-1}$, $\Theta=-8.8$ K, and $\rho=0.21$; compound **15**$^{\bullet\bullet}$: $J_\chi=-0.97\,cm^{-1}$, $\Theta=-0.7$ K, and $\rho=0.05$; compound **17**$^{\bullet\bullet}$: $J_\chi=-4.25\,cm^{-1}$, $\Theta=-4.5$ K, and $\rho=0.09$.

Table 2. Comparison of exchange coupling constants [cm^{-1}] obtained from fluid solution EPR (J_{EPR}) and solid-state magnetic susceptometry (J_{χ}).

	(Z)-$\mathbf{9}^{\cdot\cdot}$	(E)-$\mathbf{9}^{\cdot\cdot}$	$\mathbf{11}^{\cdot\cdot}$	$\mathbf{15}^{\cdot\cdot}$	$\mathbf{16}^{\cdot\cdot}$
$\lvert J_{EPR}\rvert$	0.05	1.02	1.20	0.50	≥ 2
J_{χ}	−0.74	−1.67	−2.52	−0.67	−4.25

perfine patterns and the parameters used in the simulation. For $\mathbf{17}^{\cdot\cdot}$, a comparison of J_{EPR} with J_{χ} is not possible because the former parameter is inaccessible, as $\mathbf{17}^{\cdot\cdot}$ resides in the fast-exchange limit on the ^{51}V hyperfine timescale. The correspondence of the data pairs runs from very similar ($\mathbf{15}^{\cdot\cdot}$) to highly divergent ((E)-$\mathbf{9}^{\cdot\cdot}$). The magnitudes of the J_{χ} values place them at the border of accessibility by susceptibility methods which is defined by $J \gtrsim 1\,\mathrm{cm}^{-1}$; the negative sign indicates antiferromagnetic coupling in all cases. The gradation reflects the extent to which the structures in fluid solution and in the crystal differ. The almost identical values J_{EPR} and J_{χ} for $\mathbf{15}^{\cdot\cdot}$ indicate near conformational invariance that is plausible in view of the fact that in the absence of unsaturation in the spacer coupling through the σ-bond system probably dominates; contributions from C_{ipso} and C_{α}–H hyperconjugation are expected to be similar in rigid and in conformationally interconverting molecules. In contrast, the large difference between J_{EPR} and J_{χ} for (Z)-$\mathbf{9}^{\cdot\cdot}$, which, please note, is also found for 1,2-di([5]trovacenyl)benzene ($\lvert J\rvert_{EPR}=0.04$, $J_{\chi}=-1.04\,\mathrm{cm}^{-1}$),[30] must be traced to the strain inherent in conformations in which the η^5-cyclopentadienyl and the bridging ethylene π systems deviate from strict orthogonality. Whereas in the crystal packing forces induce dihedral angles η^5-C_5H_4/μ-ethylene of 36.6°, (Z)-$\mathbf{9}^{\cdot\cdot}$ in fluid solution probably adopts the 90° conformation in which π conjugation and exchange coupling are minimal. This argument helps to rationalize the initially disturbing observation that exchange coupling in fluid solution is stronger for $\mathbf{15}^{\cdot\cdot}$ than for (Z)-$\mathbf{9}^{\cdot\cdot}$, despite the fact that the C_2 spacer in $\mathbf{15}^{\cdot\cdot}$ is saturated. The similar J values for $\mathbf{11}^{\cdot\cdot}$ and (E)-$\mathbf{9}^{\cdot\cdot}$ may be regarded as the outcome of two countervailing effects: $\mathbf{11}^{\cdot\cdot}$ features a spacer comprised of a single C-(sp^2) atom, yet the close distance of the [5]trovacenyl units causes torsion which impedes conjugation; in (E)-$\mathbf{9}^{\cdot\cdot}$ a two-carbon(sp^2) bridge is present but for this particular isomer a conformation possessing coplanarity of the two η^5-cyclopentadienyl rings and the bridging ethylene unit is tolerated or even preferred as gleaned from the crystal structure.

The fairly unsymmetrical structure of (Z)-$\mathbf{9}^{\cdot\cdot}$ in the crystal helps us to understand the peculiar temperature dependence of the EPR spectrum in fluid solution. As evident from Figure 4, satisfactory simulation was performed for the 15 line spectrum, recorded at 370 K with the parameter $\lvert J\rvert = 0.05\,\mathrm{cm}^{-1}$. Lowering the temperature initially led to a more pronounced expression of the alternating linewidth effect, which is already discernible in the 370 K spectrum. Ultimately, at 290 K, a 14 line spectrum emerges. These drastic changes of the hyperfine pattern arising in the narrow temperature range of 80° clearly point to an intramolecular dynamic process with attendant time-dependent modulation of the exchange coupling constant J. The EPR line width alternation has been known for a long time,[31] first having been observed for nitroxide biradicals.[31a] More recent examples include carboxylate-bridged oxovanadium(IV) dimers[31d] and 1,2-di([5]trovacenyl)benzene,[30] the latter exhibiting a structural pattern, bulk magnetic, and EPR features virtually identical to those found for (Z)-$\mathbf{9}^{\cdot\cdot}$. Conceivably, J modulation arises from twist distortions about the C_{ipso}–C_{α} bonds that fluctuate between a form similar to that present in the crystal (dihedral angles η^5-cyclopentadienyl/ethene 37°, large J) and a conformation in which the two π systems are orthogonal (small J). The 370 K spectrum could be simulated satisfactorily by using a single J value that may be regarded as the average between the two limiting J values (fast interconversion). The following expression [Eq. (2)], which includes a factor d allowing for linewidth alternation, was therefore employed.[31d,e]

$$\Delta B = a + b\{m_I(1) + m_I(2)\} + c\{m_I(1) + m_I(2)\}^2 + d\{m_I(1) - m_I(2)\}^2 \qquad (2)$$

Whereas the a, b, and c terms cover inhomogeneous linewidths (a) and the effects resulting from incomplete averaging of g and $A(^{51}\mathrm{V})$ anisotropies during tumbling motion (b and c), the d term treats the fluctuation of the exchange coupling constant J and its correlation time. In this way, the alternating line widths spectra could be reproduced well. Attempts to simulate the low-temperature 14 line spectrum (290 K, Figure 4) by merely varying $\lvert J\rvert$ failed.

The parameters $a(^{51}\mathrm{V})$, $\langle g\rangle$, a, b, c, d, and $\lvert J\rvert$ that led to the simulated trace in Figure 4 are given in the caption. In view of their large number, the uniquenes of the simulation and the precision of J thus determined are disputable. Beyond doubt, however, $\lvert J\rvert$ for (Z)-$\mathbf{9}^{\cdot\cdot}$ does fluctuate. Interestingly, it is only for *this* isomer that linewidth alternation is observed; this observation can be explained by the fact that only in the Z isomer do severe steric constraints inhibit rotation around the C_{ipso}–C_{α} bonds and J fluctuates about its mean value. In this situation and under the provision that $\lvert J\rvert \gg a(^{51}\mathrm{V})$, which is fulfilled here, transitions for which the individual $m_I(^{51}\mathrm{V})$ values in the dinuclear complex differ are broadened. This constitutes the alternating linewidth effect observed for (Z)-$\mathbf{9}^{\cdot\cdot}$ as depicted in Figure 4.

Conclusion

The three positional isomers of di([5]trovacenyl)ethene, (Z)-$\mathbf{9}^{\cdot\cdot}$, (E)-$\mathbf{9}^{\cdot\cdot}$, and $\mathbf{11}^{\cdot\cdot}$, differ in the extent to which electronic and magnetic effects are transmitted between the vanadium atoms. Differences in electrocommunication, which manifest themselves in redox splittings $\delta E_{1/2}$ of consecutive electron-transfer steps, are only measurable for reduction (0/−; −/2−). The small magnitude of the conproportionation constants derived therefrom and the extremely negative reduction potentials preclude isolation of the respective mixed valence species. Observation of redox splittings $\delta E_{1/2}$ (0/−; −/2−) for di([5]trovacenyl)ethane **15**$^{\cdot\cdot}$ and for di([5]trovacenyl)methane **17**$^{\cdot\cdot}$ reveals that electrocommunication is not confined to the presence of an unsaturated spacer.

The extent of magnetocommunication is quantified by the exchange coupling constant *J*, which can be determined through analysis and simulation of the EPR ^{51}V hyperfine pattern (fluid solution) or by magnetic susceptometry (polycrystalline sample). The pronounced differences in the magnitudes of the *J* values obtained by these alternative methods indicate that the conformations present in these two states of aggregation play a pivotal role in governing the interaction between the two spin centers, that is, the vanadium atoms. Consequently, the magnetic interaction is transmitted predominantly by means of the π orbitals of the bridge. Exchange coupling is attennuated, yet not quenched if the saturated ethane spacer is introduced; the mechanism of magnetic coupling in **15**$^{\cdot\cdot}$ can involve either a spin polarization path along the σ bonds of the probe–spacer combination or C_{ipso}–C_α–H hyperconjugation. Surprisingly large exchange coupling is exhibited by the methylene-linked complex **17**$^{\cdot\cdot}$, for which the relatively close proximity of the trovacene units and their tilted disposition renders a through-space mode of interaction possible. The very weak exchange coupling found for (*Z*)-**9**$^{\cdot\cdot}$ suggests that the π path dominates, because in (*Z*)-**9**$^{\cdot\cdot}$, due to severe steric constraints, π conjugation between the η^5-cyclopentadienyl rings and the ethene spacer is restricted. Steric hindrance in (*Z*)-**9**$^{\cdot\cdot}$ prevents full rotation of the trovacenyl units about the C_{ipso}–C_{spacer} bonds. Instead, torsional motion between two limiting dihedral angles η^5-C_5H_4/-$(CHR)_2$-, passing through a 90° conformation with zero π conjugation, are conceivable. The attendant fluctuation in the exchange coupling constant *J* manifests itself in the alternating line width effect which the EPR spectra of (*Z*)-**9**$^{\cdot\cdot}$ show in the temperature range $370 \geq T \geq 290$ K and which is peculiar to this isomer.

Experimental Section

General: All chemical manipulations were performed in an atmosphere of purified dinitrogen or argon in dry and degassed solvents employing standard Schlenk techniques. $TiCl_3$ was commercially available and was used as received. Physical measurements were carried out with the instruments described previously.[1] Crystallographic data are given in Table 3. Treatment of hydrogen atoms: for (*E*)-**9**$^{\cdot\cdot}$, isotropic refinement; for (*Z*)-**9**$^{\cdot\cdot}$, riding model; for **11**$^{\cdot\cdot}$, isotropic refinement, 7-ring H calculated; for **12**$^{\cdot}$ refined, disorder calculated; and for **15**$^{\cdot\cdot}$ isotropic refinement. Absorption corrections were not performed.

Acetyl-[5]trovacene (8$^{\cdot}$): Acetyl-η^5-cyclopentadienyl)tetracarbonylvanadium[32] (1.58 g, 5.85 mmol) was heated under reflux in cycloheptatriene (25 mL) for 24 h. After cooling to ambient temperature the volatiles were removed in vacuo. The dark residue was redissolved in toluene and subjected to column chromatography (Al_2O_3, 3% H_2O, 3×40 cm). Elution of a green zone by toluene/THF (50:1) and removal of the solvent in vacuo afforded the product as an amorphous green solid. Yield: 0.85 g (3.41 mmol), 58%; MS (70 eV, EI): *m/z* (%): 249 (100) [M^+], 158 (6) [$M^+-C_7H_7$], 91 (37) [$C_7H_7^+$], 67 (16) [$C_5H_6^+$], 51 (6) [V^+]; elemental analysis calcd (%) for $C_{14}H_{14}OV$ (249.20): C 67.47, H 5.66; found: C 68.11, H 6.27; IR (toluene): $\tilde{\nu} = 1678$ cm^{-1} (C=O); EPR (X-band, toluene): $g_{iso} = 1.9865$, $a(^{51}V) = -7.30$ mT (298 K), $g_\parallel = 2.0027$, $g_\perp = 1.9780$, $A_\parallel = -1.26$ mT, $A_\perp = -10.32$ mT (100 K); cyclic voltammetry (DME/0.1 M Bu_4NClO_4, −35 °C, $\nu = 100$ mV s^{-1} vs SCE): $E_{1/2}(+,0) = 0.43$ V, $\Delta E_p = 53$ mV; $E_{pa} = 1.13$ V; $E_{1/2}(0,-) = -2.21$ V, $\Delta E_p = 55$ mV, $E_{pc} = -2.74$ V.

2,3-Di([5]trovacenyl)-2-butenes (*Z*)-9$^{\cdot\cdot}$ and (*E*)-9$^{\cdot\cdot}$: [$TiCl_3(dme)_{1.5}$][12d] (1.34 g, 4.56 mmol) and Zn(Cu)[12d] (1.16 g, 17.6 mmol) were heated to reflux in DME (50 mL) for 2 h. After cooling to room temperature a solution of **8**$^{\cdot}$ (0.27 g, 1.08 mmol) in DME (8 mL) was added rapidly to the black suspension and the mixture was refluxed for 20 h. After cooling to

Table 3. Crystallographic and refinement data.

	(*E*)-**9**$^{\cdot\cdot}$	(*Z*)-**9**$^{\cdot\cdot}$	**11**$^{\cdot\cdot}$	**12**$^{\cdot\cdot}$	**16**$^{\cdot\cdot}$
size [mm^{-3}]	0.30×0.27×0.09	0.35×0.30×0.20	0.45×0.30×0.10	0.36×0.19×0.08	0.30×0.15×0.15
crystal system	monoclinic	monoclinic	monoclinic	monoclinic	monoclinic
space group	$P2_1/n$	$P2_1/c$	$P2_1/c$	$P2_1/c$	$P2_1/n$
Z	4	4	4	8	4
a [Å]	11.0352(8)	10.8650(6)	21.5635(11)	6.6010(6)	10.8966(10)
b [Å]	8.0664(7)	19.3338(8)	7.7503(4)	25.1421(17)	8.0248(4)
c [Å]	12.8284(9)	13.1973(8)	11.7382(7)	12.6856(12)	22.9874(19)
β [°]	113.646(7)	96.644(6)	91.821(7)	96.272(11)	102.744(10)
V [Å^3]	1046.04(14)	2753.6(3)	1960.74(18)	2092.7(3)	1960.6(3)
formula	$C_{14}H_{14}V$	$C_{35}H_{36}V_2$	$C_{26}H_{24}V_2$	$C_{13}H_{12}OV$	$C_{26}H_{26}V_2$
M_r	233.19	558.52	438.33	235.17	440.35
ρ_{calcd} [Mg m^{-3}]	1.481	1.347	1.485	1.493	1.492
μ [mm^{-1}]	0.906	0.701	0.962	0.913	0.962
F(000)	484	1168	904	968	912
θ range [°]	2.06–26.01	1.88–25.89	2.79–25.00	2.29–25.94	1.82–25.87
hkl index ranges	−13/13, −9/9, −14/15	−13/13, −23/23, −16/16	−25/25, −9/9, −13/13	−8/8, −30/29, −14/15	−13/13, −9/9, −28/27
reflns collected	7866	21449	12998	12815	14926
independent reflns	1964 [*R*(int) = 0.0200]	5330 [*R*(int) = 0.0440]	3397 [*R*(int) = 0.0491]	4042 [*R*(int) = 0.0500]	3794 [*R*(int) = 0.0721]
completeness	96.9%	99.6%	98.5%	99.7%	99.8%
obsd reflns [$I > 2\sigma(I)$]	1715	3692	2772	2732	2385
reflns used	1964	5330	3397	4042	3794
largest diff peak/hole [e Å^{-3}]	0.259/−0.189	0.389/−0.267	0.894/−0.353	0.294/−0.252	0.580/−0.331
parameters	181	376	294	405	357
GOF on F^2	1.048	0.904	1.221	0.899	0.888
*wR*2 (all data)	0.0685	0.0779	0.1318	0.0710	0.0966
*R*1 [$I > 2\sigma(I)$]	0.0251	0.0314	0.0528	0.0309	0.0388

ambient temperature the green-black suspension was diluted with hexane (40 mL) and filtered through a 2 cm layer of celite. The green filtrate was evaporated to dryness in vacuo and the dark residue redissolved in toluene and kept at ambient temperature for several hours. A dark green precipitate of (*E*)-**9**$^{\bullet\bullet}$ was collected by fitration, which was recrystallized from toluene, washed twice with diethyl ether, and dried in vacuo. Yield: 0.08 g (0.15 mmol), 28 %. The toluene filtrate of (*E*)-**9**$^{\bullet\bullet}$ was subjected to column chromatography (Al_2O_3, 2×40 cm, toluene). The first gray-green fraction containing (*Z*)-**9**$^{\bullet\bullet}$ was collected, the solvent removed, and the blue-green residue was washed with hexane. Yield: 0.15 g (0.32 mmol, 60 %) of (*Z*)-**9**$^{\bullet\bullet}$. A second, light green fraction was eluted, which yielded a very small amount of (*E*)-**9**$^{\bullet\bullet}$. For both compounds single crystals suitable for X-ray diffraction were obtained from solutions in toluene.

Data for (*E*)-**9**$^{\bullet\bullet}$: MS (70 eV, EI): *m/z* (%): 466 (100) [M^+], 375 (67) [$M^+ - C_7H_7$], 233 (35) [M^{++}], 116 (19) [$C_5H_5V^+$]; elemental analysis calcd (%) for $C_{28}H_{28}V_2$ (466.41): C 72.11, H 6.05; found: C 71.87, H 5.81; IR (KBr): $\tilde{\nu} = 1639$, 1618 cm^{-1} (C=C); for CV, EPR, and magnetic susceptometry data see text.

Data for (*Z*)-**9**$^{\bullet\bullet}$: MS (70 eV, EI): *m/z* (%): 466 (100) [M^+], 375 (67) [$M^+ - C_7H_7$], 233 (35) [M^{++}], 116 (19) [$C_5H_5V^+$]; elemental analysis calcd (%) for $C_{28}H_{28}V_2$ (466.41): C 72.11, H 6.05; found: C 72.60, H 6.20; IR (KBr): $\tilde{\nu} = 1638$, 1618 cm^{-1} (C=C); for CV, EPR, and magnetic susceptometry data see text.

1,1-Di([5]trovacenyl)ethene (11$^{\bullet\bullet}$): *n*-Butyllithium (1.6 M in hexane, 1.2 mL, 1.93 mmol) was added to a solution of trovacene **1**$^{\bullet}$[33b] (0.4 g, 1.93 mmol) in THF/diethyl ether (1:1, 50 mL) at −10 °C and the mixture was stirred at ambient temperature overnight. Compound **8**$^{\bullet}$ (0.45 g, 1.81 mmol) in THF (10 mL) was added dropwise and stirring was continued for several hours. After cooling to 0 °C, the mixture was hydrolyzed with 2 M HCl (2 mL) and stirred at room temperature for 4.5 h. The residue from solvent removal in vacuo was redissolved in benzene and the solution was dried over Na_2SO_4. Filtration through silica gel (2×8 cm) afforded a blue-green solution, which was subjected to column chromatography (Al_2O_3, 2 % H_2O, 2×39 cm, benzene). The first violet fraction contained unreacted trovacene **1**$^{\bullet}$, followed by a weak yellow-green band. Finally, the target compound **11**$^{\bullet\bullet}$ was obtained from a gray-blue fraction upon evaporation in vacuo. The gray residue was washed with diethyl ether and hexane. Yield of **11**$^{\bullet\bullet}$: 0.05 g (0.11 mmol, 6 % based on **8**$^{\bullet}$). Single crystals suitable for X-ray diffraction were grown from a solution in benzene layered with hexane. MS (70 eV, EI): *m/z* (%): 438 (100) [M^+], 347 (42) [$M^+ - C_7H_7$], 219 (13) [M^{++}], 116 (46) [$C_5H_5V^+$], 78 (35) [$C_6H_6^+$]; elemental analysis calcd (%) for $C_{26}H_{24}V_2$ (438.359): C 71.24, H 5.52; found: C 70.51, H 5.86; IR (KBr): $\tilde{\nu} = 3105$, (CH_2), 1650, 1580 (C=C), 876 cm^{-1} (C=CH_2); for CV, EPR, and magnetic susceptometry data see text.

Hydroxymethyl-[5]trovacene (14$^{\bullet}$): Solid $NaBH_4$ (0.38 g, 10 mmol) was added portionwise to a solution of compound **12**$^{\bullet}$[1] (1.03 g, 4.38 mmol) in methanol (50 mL) at 0 °C. After 10 min the color of the solution changed from dark green to violet. Stirring was continued for 10 min, then HCl (0.5 N, 25 mL) was added. The mixture was extracted with benzene/diethyl ether. The combined organic phases were washed with water and dried over Na_2SO_4, and the solvent was removed in vacuo. Crude **14**$^{\bullet}$ was obtained as a violet solid (1 g, 4.21 mmol, 96 %), which was sufficiently pure for subsequent reactions. Further purification was achieved by chromatography (silica gel, toluene/diethyl ether (20–10:1)) and recrystallization from hexane. MS (70 eV, EI): *m/z* (%): 237 (63) [M^+], 159 (100) [$M^+ - 78$], 129 (37) [$C_6H_6V^+$], 116 (7) [$C_5H_5V^+$], 91 (30) [$C_7H_7^+$], 67 (26) [$C_5H_6^+$], 51 (14) [V^+]; elemental analysis calcd (%) for $C_{13}H_{14}OV$ (237.189): C 65.83, H 5.95; found: C 64.65, H 5.63; IR (KBr): $\tilde{\nu} = 3213$ (O–H), 1314 cm^{-1} (C–O); EPR (X-band, MTHF): $g_{iso} = 1.9832$, $a(^{51}V) = -7.15$ mT (294 K, $f = 9.2449$ GHz), $g_{\parallel} = 2.0008$, $g_{\perp} = 1.9744$, $A_{\parallel} = -1.18$ mT, $A_{\perp} = -10.13$ mT (124 K, f = 9.2498 GHz); cyclic voltammetry (DME/0.1 M Bu_4NClO_4, −35 °C, $\nu = 100$ mV s^{-1} vs SCE): $E_{1/2}(+,0) = 0.27$ V, $\Delta E_p = 73$ mV; $E_{pa} = 1.04$ V; $E_{1/2}(0,-) = -2.46$ V, $\Delta E_p = 71$ mV.

1,2-Di([5]trovacenyl)ethane (15$^{\bullet\bullet}$): *n*-Butyllithium (1.6 M in hexane, 1.2 mL, 1.88 mmol) was added to a cooled (−60 °C) suspension of $TiCl_3$ (0.29 g, 1.88 mmol) in DME (20 mL) and the mixture stirred for 30 min. Triethylamine (0.26 mL, 1.88 mmol) was added to the dark suspension and finally a suspension of the lithium salt of alcohol **14**$^{\bullet}$ [prepared previously by adding *n*-butyllithium (1.6 M in hexane, 1.14 mL, 1.83 mmol) to a solution of **14**$^{\bullet}$ in DME (25 mL) at −10 °C] was added rapidly. The black suspension was stirred at room temperature for 1.5 h and heated under reflux for an additional 2 h. After cooling to ambient temperature, the mixture was poured into aqueous sodium acetate (15 %, 150 mL). The resulting green-black suspension was extracted four times with toluene (250 mL in total). The combined organic extracts were washed with water, dried with Na_2SO_4, and concentrated in vacuo. The product precipitated from the violet solution after several days and was recrystallized from hot toluene yielding 80 mg of **15**$^{\bullet\bullet}$. An additional crop of 60 mg was obtained by stirring the aqueous phase with toluene overnight and working up the organic phase as described above. Combined yield: 0.14 g (0.32 mmol), 35 %. Single crystals suitable for X-ray diffraction were grown from a saturated solution in benzene. MS (70 eV, EI): *m/z* (%): 440 (100) [M^+], 349 (68) [$M^+ - C_7H_7$], 220 (63) [M^{++}], 142 (32) [$C_7H_7V^+$], 129 (7) [$C_6H_6V^+$], 116 (19) [$C_5H_5V^+$], 91 (35) [$C_7H_7^+$], 51 (36) [V^+]; elemental analysis calcd (%) for $C_{26}H_{26}V_2$ (440.375): C 70.91, H 5.95; found: C 70.73, H 5.91; IR (KBr): $\tilde{\nu} = 2918$, 2855 cm^{-1} (CH_2); for CV, EPR, and magnetic susceptometry data see text.

μ-Di(η^5-cyclopentadienyl)methanebis[(tetracarbonyl)vanadium] (16): A mixture of $V(CO)_6$[34] (1.894 g, 8.65 mmol) and freshly prepared dicyclopentadienylmethane[35] (0.614 g, 4.26 mmol) was heated under reflux in methylcyclohexane (50 mL) for 4 h. After cooling to ambient temperature the mixture was filtered through a 2 cm layer of celite and evaporated to dryness in vacuo. The residue was subjected to column chromatography {Al_2O_3 (2×20 cm, toluene/CH_2Cl_2 (9:1)}. Elution of a yellow zone and evaporation of the eluent in vacuo afforded 457 mg (0.98 mmol, 23 %) of the product **16** as an orange oil which was used in the subsequent reaction without further purification. EI-MS (70 eV): *m/z* (%): 468 (6) [M^+], 356 (14) [$M^+ - 4CO$], 328 (38) [$M^+ - 5CO$], 300 (100) [$M^+ - 6CO$], 272 (50) [$M^+ - 7CO$], 244 (43) [$M^+ - 8CO$], 193 (16) [$M^+ - 8CO - V$], 122 (11) [$M^{++} - 8CO$], 116 (13) [$C_5H_5V^+$], 51 (23) [V^+]; IR (nujol mull): $\tilde{\nu} = 2022$, 1924 cm^{-1} (C=O).

Di([5]trovacenyl)methane (17$^{\bullet\bullet}$): Compound **16** (452 mg, 0.97 mmol) was heated under reflux in cycloheptatriene (30 mL) for 30 h. The residue from filtration and evaporation of the solvent in vacuo was subjected to column chromatography (Al_2O_3, 2×35 cm, toluene/THF 99:1). Elution of a pale violet zone and concentration to dryness in vacuo afforded a violet powder, which was recrystallized from hot toluene. The target compound **17**$^{\bullet\bullet}$ precipitated as light violet leaflets in a yield of 33 mg (0.077 mmol, 8 %). EI-MS (70 eV): *m/z* (%): 426 (100) [M^+], 213 (17) [M^{++}], 142 (3) [$C_7H_7V^+$], 91 (7) [$C_7H_7^+$]; elemental analysis calcd (%) for $C_{25}H_{24}V_2$ (426.347): C 70.43, H 5.67; found: C 69.97, H 5.81.

Vinyl[5]trovacene (13$^{\bullet}$): A solution of compound **12**$^{\bullet}$ (0.36 g, 1.53 mmol) and $[(C_5H_5)_2Ti(CH_3)_2]$[11b] (0.79 g, 3.83 mmol) in THF (40 mL) was heated to 65 °C for 20 h under exclusion of light. After cooling to room temperature the solvent was removed in vacuo. The residue was extracted into toluene (4 mL) and filtered through Al_2O_3 (3 % H_2O, 2×10 cm, toluene). The dark green filtrate was evaporated to dryness and the residue was redissolved in methyl cyclohexane (5 mL) and subjected to chromatography at Al_2O_3 (3 % H_2O, 2×20 cm). A gray-violet zone containing the product was eluted with methyl cyclohexane/benzene (30:1). The eluate was concentrated to a volume of 1.5 mL and stored at 4 °C overnight. Compound **13**$^{\bullet}$ precipitated as a violet fibrous material (0.11 g, 0.47 mmol) in a yield of 31 %. MS (70 eV, EI): *m/z* (%): 233 (100) [M^+], 155 (8) [$M^+ - 78$], 142 (8) [$C_7H_7V^+$], 129 (10) [$C_6H_6V^+$], 116 (3) [$C_5H_5V^+$], 51 (34) [V^+]; elemental analysis calcd (%) for $C_{14}H_{14}V$ (233.207): C 72.11, H 6.05; found: C 71.50, H 5.95; IR (KBr): $\tilde{\nu} = 1631$ (C=C), 893 cm^{-1} (C=CH_2); EPR (X-band, toluene): $g_{iso} = 1.9828$, $a(^{51}V) = -7.19$ mT (295 K, $f = 9.2444$ GHz), $g_{\parallel} = 2.0008$, $g_{\perp} = 1.9738$, $A_{\parallel} = -1.16$ mT, $A_{\perp} = -10.21$ mT (122 K, $f = 9.2470$ GHz); cyclic voltammetry (DME/0.1 M Bu_4NClO_4, −35 °C, $\nu = 100$ mV s^{-1} vs SCE): $E_{1/2}(+,0) = 0.27$ V, $\Delta E_p = 74$ mV; $E_{pa} = 1.11$ V; $E_{1/2}(0,-) = -2.47$ V, $\Delta E_p = 75$ mV.

Acknowledgements

This work was supported by the Deutsche Forschungsgemeinschaft and the Fonds der Chemischen Industrie.

---

[1] C. Elschenbroich, J. Plackmeyer, M. Nowotny, K. Harms, J. Pebler, O. Burghaus, *Inorg. Chem.* **2005**, *44*, 955.

[2] C. A. Creutz, H. Taube, *J. Am. Chem. Soc.* **1969**, *91*, 3988.

[3] a) T. J. Meyer in *Comprehensive Coordination Chemistry I* (Eds.: G. Wilkinson, R. D. Gillard, J. A. McCleverty), Pergamon, Oxford, **1987**, pp. 331–384; J. F. Endicott, C. A. Creutz, B. S. Bunschwig, N. Sutin, D. Gatteschi, R. Sessoli in *Comprehensive Coordination Chemistry II, Vol. 7* (Eds.: J. A. McCleverty, T. J. Meyer, M. Fujita, A. Powell, C. A. Creutz), Elsevier, Amsterdam, **2004**, Chapter 7.11–7.13; b) D. Astruc, *Electron Transfer and Radical Processes in Transition-Metal Chemistry*, VCH, New York, **1995**; c) R. J. Crutchley, *Adv. Inorg. Chem.* **1994**, *41*, 273; d) J. A. McCleverty, M. D. Ward, *Acc. Chem. Res.* **1998**, *31*, 842; e) M. D. Ward, J. A. McCleverty, *J. Chem. Soc. Dalton Trans.* **2002**, 275; f) J. Cano, E. Ruiz, S. Alvarez, M. Verdaguer, *Comments Inorg. Chem.* **1998**, *20*, 27; g) J. S. Miller, A. J. Epstein, *Angew. Chem.* **1994**, *106*, 399; *Angew. Chem. Int. Ed. Engl.* **1994**, *33*, 385; h) O. Kahn, *Molecular Magnetism*, VCH, Weinheim, **1993**; i) S. Barlow, D. O'Hare, *Chem. Rev.* **1997**, *97*, 637; j) F. Paul, C. Lapinte in *Unusual Structures and Physical Properties in Organometallic Chemistry* (Eds.: M. Gielen, R. Willem, B. Wrackmeyer), Wiley, Chichester, **2002**, pp. 219–295; k) E. Ruiz, A. Rodriguez-Fortea, S. Alvarez, *Inorg. Chem.* **2003**, *42*, 4881.

[4] Trovacene = (**tro**pylium)**va**nadium(**c**yclop**en**tadi**e**nyl); [5]trovacenyl derivatives are functionalized at the C_5 ligand and [7]trovacenyl derivatives at the C_7 ligand.

[5] C. Elschenbroich, O. Schiemann, O. Burghaus, K. Harms, *J. Am. Chem. Soc.* **1997**, *119*, 7452.

[6] C. Elschenbroich, O. Schiemann, O. Burghaus, K. Harms, J. Pebler, *Organometallics* **1999**, *18*, 3273.

[7] C. Elschenbroich, J. Plackmeyer, K. Harms, O. Burghaus, J. Pebler, *Organometallics* **2003**, *22*, 3367.

[8] C. Elschenbroich, M. Wolf, O. Schiemann, K. Harms, O. Burghaus, J. Pebler, *Organometallics* **2002**, *21*, 5810.

[9] a) A. Kasahara, T. Izumi, *Chem. Lett.* **1978**, 21; b) T. Y. Dong, T. J. Ke, S. M. Peng, S. K. Yeh, *Inorg. Chem.* **1989**, *28*, 2103; c) A. C. Ribou, J. P. Launay, M. L. Sachtleben, H. Li, C. W. Spangler, *Inorg. Chem.* **1996**, *35*, 3735; d) Y. J. Chen, D. S. Pan, C. F. Chiu, J. X. Su, S. J. Lin, K. S. Kwan, *Inorg. Chem.* **2000**, *39*, 953.

[10] a) C. F. Chiu, M. Song, B. H. Chen, K. S. Kwan, *Inorg. Chim. Acta* **1997**, *266*, 73; b) M. Sato, Y. Kawata, A. Kudo, A. Iwai, H. Saitoh, S. Ochiai, *J. Chem. Soc. Dalton Trans.* **1998**, 2215.

[11] a) N. A. Petasis, E. I. Bzowej, *J. Am. Chem. Soc.* **1990**, *112*, 6392; b) K. Claus, H. Bestian, *Justus Liebig Ann. Chem.* **1962**, *654*, 8.

[12] a) J. E. McMurry, M. P. Fleming, *J. Am. Chem. Soc.* **1974**, *96*, 4708; b) J. E. McMurry, M. P. Fleming, K. L. Kees, L. R. Krepski, *J. Org. Chem.* **1978**, *43*, 3255; c) J. E. McMurry, *Chem. Rev.* **1989**, *89*, 1513; d) T. Lectka in *Active Metals* (Ed.: A. Fürstner), VCH, Weinheim, **1996**; e) D. Lenoir, H. Burghard, *J. Chem. Res. Synop.* **1980**, 396.

[13] J. Plackmeyer, Ph.D. thesis, Philipps-Universität Marburg (Germany), **2001**.

[14] F. S. Arimoto, A. C. Haven, *J. Am. Chem. Soc.* **1955**, *77*, 6295.

[15] K. L. Rinehart, P. A. Kittle, A. F. Ellis, *J. Am. Chem. Soc.* **1960**, *82*, 2082.

[16] The original determination of the structure of $[(C_7H_7)V(C_5H_5)]$ (**1**$^\bullet$) (G. Engebretson, R. E. Rundle, *J. Am. Chem. Soc.* **1963**, *85*, 481) suffered from a high discrepancy factor, $R = 0.186$. Our data were compared with a more thoroughly refined structure of **1**$^\bullet$ ($R = 0.046$), which has been forthcoming recently: K. A. Lyssenko, M. Yu. Antipin, S. Yu. Ketkov, *Russ. Chem. Bull.* **2001**, *50*, 130.

[17] W. H. Morrison, S. Krogsrud, D. N. Hendrickson, *Inorg. Chem.* **1973**, *12*, 1998.

[18] a) R. E. Richardson, H. Taube, *Inorg. Chem.* **1981**, *20*, 1278; b) R. E. Richardson, H. Taube, *Coord. Chem. Rev.* **1984**, *60*, 107; c) D. M. D'Alessandro, R. F. Keene, *Dalton Trans.* **2004**, 3950.

[19] a) N. S. Hush, *Coord. Chem. Rev.* **1985**, *64*, 135; b) J. P. Launay, *Chem. Soc. Rev.* **2001**, *30*, 386; c) A.-C. Ribou, J.-P. Launay, M. L. Sachtleben, H. Li, C. W. Spangler, *Inorg. Chem.* **1996**, *35*, 3735.

[20] a) R. J. Crutchley, *Adv. Inorg. Chem.* **1994**, *41*, 273; b) M. L. Naklicki, C. A. White, L. L. Plante, C. E. B. Evans, R. J. Crutchley, *Inorg. Chem.* **1998**, *37*, 1880; c) P. J. Mosher, G. P. A. Yap, R. J. Crutchley, *Inorg. Chem.* **2001**, *40*, 1189; d) M. D. E. Forbes, J. D. Ball, N. I. Avdievich, *J. Am. Chem. Soc.* **1996**, *118*, 4707.

[21] EPR fitting and simulation program "SIMEPR", O. Burghaus, University of Marburg, available on request; O. Burghaus, Proceedings of the Joint 29th AMPERE—13th ISMAR International Conference, Technische Universität Berlin, **1998**, *Magnetic Resonance and Related Phenomena, Vol. II*, p. 1186; see also references [31 d,e].

[22] a) F. J. Adrian, E. L. Cochran, V. A. Bowers, *Free Radicals in Inorganic Chemistry*, American Chemical Society, Washington, DC, **1962**; b) A. A. Bothner-By, *Adv. Magn. Reson.* **1965**, *1*, 195.

[23] To the extent that exchange coupling and electron transfer share a common barrier, the observation of long-range intervalence electron tunneling through fully saturated systems is inspiring: C. A. Stein, N. A. Lewis, G. Seitz, *J. Am. Chem. Soc.* **1982**, *104*, 2596.

[24] C. Elschenbroich, J. Koch, J. Schneider, B. Spangenberg, *J. Organomet. Chem.* **1986**, *317*, 41.

[25] a) C. Heller, H. M. McConnell, *J. Chem. Phys.* **1960**, *32*, 1575; b) J. R. Morton, *Chem. Rev.* **1964**, *64*, 453; c) D. Lazdins, M. Karplus, *J. Chem. Phys.* **1966**, *44*, 1600.

[26] B. F. Fieselmann, D. N. Hendrickson, G. D. Stucky, *Inorg. Chem.* **1978**, *17*, 1841.

[27] a) J. A. McCleverty, M. D. Ward, *Acc. Chem. Res.* **1998**, *31*, 842; b) P. K. A. Shonfield, A. Behrendt, J. C. Jeffery, J. P. Maher, J. A. McCleverty, E. Psillakis, M. D. Ward, C. Western, *J. Chem. Soc. Dalton Trans.* **1999**, 4341.

[28] a) F. Paul, C. Lapinte, *Coord. Chem. Rev.* **1998**, *178/180*, 427; b) F. Paul, C. Lapinte in *Unusual Structures and Physical Properties in Organometallic Chemistry* (Eds.: M. Gielen, R. Willem, B. Wrackmeyer), Wiley, Chichester, **2002**; c) S. Roue, C. Lapinte, T. Battaile, *Organometallics* **2004**, *23*, 2538.

[29] a) K. McGregor, D. J. Hodgson, W. E. Hatfield, *Inorg. Chem.* **1973**, *12*, 731; b) J. A. van Santen, A. J. van Duynefeld, R. L. Carlin, *Inorg. Chem*, **1980**, *19*, 2152; c) P. D. W. Boyd, S. Mitra, C. L. Raston, G. L. Rowbottom, A. H. White, *J. Chem. Soc. Dalton Trans.* **1981**, 13.

[30] O. Schmiemann, Ph.D. Thesis, Marburg, **1998**.

[31] a) R. Brière, R. M. Dupeyre, H. Lemaire, C. Morat, A. Rassat, P. Rey, *Bull. Chim. Soc. Fr.* **1965**, 3290; b) G. R. Luckhurst, *Mol. Phys.* **1966**, *10*, 543; c) S. H. Glarum, J. H. Marshall, *J. Chem. Phys.* **1967**, *47*, 1374; d) A. Hudson, G. R. Luckhurst, *Chem. Rev.* **1969**, *69*, 191; e) D. Collison, F. E. Mabbs, S. S. Turner, *J. Chem. Soc. Faraday Trans.* **1993**, *89*, 3705; f) F. E. Mabbs, *Chem. Soc. Rev.* **1993**, *22*, 313.

[32] a) E. O. Fischer, K. Plesske, *Chem. Ber.* **1960**, *93*, 1006; b) D. Rehder, M. Hoch, *Chem. Ber.* **1988**, *121*, 1541.

[33] a) C. Floriani, V. Mange, *Inorg. Synth.* **1991**, *28*, 263. C. Floriani, *J. Chem. Soc. Dalton Trans.* **1976**, 1046; b) R. B. King, F. G. A. Stone, *J. Am. Chem. Soc.* **1959**, *81*, 5263.

[34] J. E. Ellis, R. A. Faltynek, G. L. Rochfort, R. E. Stevens, G. A. Zank, *Inorg. Chem.* **1980**, *19*, 1082.

[35] N. E. Schore, C. S. Ilenda, M. A. White, H. E. Bryndza, M. G. Matturro, R. G. Bergman, *J. Am. Chem. Soc.* **1984**, *106*, 7451–7461.

Received: May 3, 2005